RSC Advances

ROYAL SOCIETY OF CHEMISTRY

REVIEW

View Article Online
View Journal | View Issue

Check for updates

Cite this: *RSC Adv.*, 2025, **15**, 45245

Exploring recent advances and synthesis strategies in conductive polymers and their composites in supercapacitor systems: a comprehensive review

Ahmed Aldulaimi,[a] Shakir Mahmood Saeed,[b] Soumya V. Menon,*[c]
Ruya Yilmaz Saber,[d] Subhashree Ray,[e] Karthikeyan Jayabalan,[f] Aashna Sinha,[g]
Renu Sharma,[h] Waam Mohammed Taher*[i] and Mariem Alwan[j]

Received 2nd September 2025
Accepted 24th October 2025

DOI: 10.1039/d5ra06603d

rsc.li/rsc-advances

The expansion of industry has led to increased environmental pollution and irreparable damage to the ecosystem. Supercapacitors (hybrid capacitors) have been introduced as renewable energy sources with high power density and energy density. Conducting polymers were introduced as pseudocapacitor electroactive materials. Conducting polymers have advantages, including high stability during alternating charge–discharge cycles, high conductivity, and corrosion resistance. Preparing conductive polymer-based composites with other electroactive materials (MOFs, TMS, C, TMO, and MXene) due to synergistic effects leads to the achievement of high-performance hybrid electrode materials. The electrochemical performance of these composites varied depending on the type of electroactive materials (MOFs, TMS, C, TMO, and MXene), the type of conductive polymer, and the synthesis method. In this study, an attempt was made to provide a basis for researchers to conduct innovative studies by reviewing the synthesis methods, supercapacitor studies conducted on various conductive polymers, and composites based on conductive polymers.

1. Introduction

The gases produced by thermal power plants and fossil fuel combustion have caused irreparable environmental damage.[1–3] Therefore, renewable energy sources are essential for the energy supply for industry.[3–5] Energy storage devices, including supercapacitors,[6] fuel cells,[7,8] and various types of lithium batteries[9] have been investigated as renewable energy sources over the last decade.[10,11] Supercapacitor devices are innovative energy storage systems that operate in a manner intermediate between a battery and a capacitor. In other words, supercapacitors offer the advantages of both a battery and a capacitor simultaneously.[12–14] Conventional capacitors have lower energy density than batteries.[15–19] Supercapacitors overcome the limitations of other energy storage systems (batteries and capacitors) by combining the characteristics of a battery and a capacitor.[20,21] Supercapacitor devices consist of three main components: the current collector,[22] electrolyte,[23] and electrode material.[24] Intelligent selection of each supercapacitor component (current collector, electrolyte, and electrode materials) plays a role in the final behavior of efficient supercapacitor devices.[18,25,26] The type of electrode material is influential in determining the type of supercapacitor performance (pseudocapacitor, hybrid capacitors, and EDLC).[27–30] Carbon materials, including GO,[31] rGO,[32] CNT,[33] AC,[34] and aerogels,[35] have EDLC behavior. Metal oxides,[36] metal sulfides,[37] quantum dots,[38] and conducting polymers have pseudocapacitor behavior.[39] Pseudocapacitor electrode materials have lower power density than EDLC electrode materials.[40,41] To overcome the limitations of pseudocapacitors and EDLCs, the hybrid capacitor device was designed and fabricated, which simultaneously has high energy density and power density.[42,43] Conductive polymers, as pseudocapacitors electrode materials, have metal conductive properties and polymer properties.[44] Researchers prepared bicomponent or multicomponent composites of CP with other materials (MOFs, TMS, C, and TMO) to make a hybrid supercapacitor device.[45–47] Conductive polymers as electroactive

---

[a] *Department of Pharmacy, Al-Zahrawi University, Karbala, Iraq*

[b] *College of Pharmacy, Alnoor University, Nineveh, Iraq*

[c] *Department of Chemistry and Biochemistry, School of Sciences, JAIN (Deemed to be University), Bangalore, Karnataka, India. E-mail: v.menon.in@gmail.com; v.soumya@jainuniversity.ac.in*

[d] *Medical Device Technology Engineering, Al-Turath University, Al Mansour, Baghdad 10013, Iraq*

[e] *Department of Biochemistry, IMS and SUM Hospital, Siksha 'O' Anusandhan (Deemed to be University), Bhubaneswar, Odisha-751003, India*

[f] *Department of Chemistry, Sathyabama Institute of Science and Technology, Chennai, Tamil Nadu, India*

[g] *School of Applied and Life Sciences, Division of Research and Innovation, Uttaranchal University, Dehradun, Uttarakhand, India*

[h] *Department of Chemistry, University Institute of Sciences, Chandigarh University, Mohali, Punjab, India*

[i] *College of Nursing, National University of Science and Technology, Dhi Qar, Iraq. E-mail: waam_mohammed@nust.edu.iq*

[j] *Pharmacy College, Al-Farahidi University, Iraq*

materials have limitations, including low stability during the GCD method and volume expansion and contraction, which can be overcome by composites with other electroactive materials, including GO, CNT, *etc.*[48–51] Also, other composites based on conductive polymers with metal oxides or sulfides, MOFs, and quantum dots have been synthesized and reported as two-component or multi-component composites to achieve hybrid electrode materials.[52–54] In this study, the performance of conductive polymers and their composites was reviewed as electroactive materials in supercapacitors. In other words, supercapacitor studies conducted on conductive polymer-based composites, such as composites of conductive polymer with carbon materials, MOFs, metal oxides, metal sulfides, and MXene, were reported in this review study. The effect of composite components (composites prepared from conductive polymers with MOF, metal oxides, metal sulfides, carbon materials, and quantum dots) in achieving efficient hybrid electrode materials was discussed and investigated by examining various synthesis methods and other parameters. Therefore, this review provides researchers with a broad perspective for conducting innovative research.

2. Energy storage devices

Supercapacitors were referenced by General Electric in 1957, followed by devices patented by SOHIO in 1960–1970. Further developments were reported by NEC, Panasonic (Japan), and other companies in 1996.[55–57] Therefore, the supercapacitor has been investigated in many research studies as an efficient and innovative energy storage technology.[58] Supercapacitors, as an energy storage system with long lifespan, high power, and excellent performance over a wide temperature range, have many applications in various industries.[59] Supercapacitors were used in the electric vehicle, forklift, and crane industries. Also, supercapacitors have been utilized as energy storage sources in various applications, including wind turbines, electronic devices (such as mobile phones and tablets),[60] solar energy systems,[61] medical devices,[62,63] camera flashes,[64] and UPS systems.[65] Supercapacitor devices possess performance between capacitors and batteries. According to the Ragone diagram, batteries have a higher energy density than capacitors; however, batteries have a lower power density. The performance of batteries in industry is limited due to the low stability of charge and discharge cycles, resource limitations (lithium salt), and expensive storage conditions.[66] The classification of supercapacitors into three main groups corresponds to the electrode material.[67]

2.1. Electric double layer capacitor (EDLC)

In EDLCs, the specific capacitance corresponds to the storage of electrostatic charge in the interface of the electrode and electrolyte. The performance of EDLCs corresponds to the specific surface area of the electrode materials and has a low energy density.[68] EDLCs consist of carbon material types, including activated carbon,[69] CNT,[70] GO,[6] rGO, and MXene.[71] The structure of EDLCs was first proposed by Helmholtz as shown in Fig. 1a.[72] According to the Helmholtz model, two layers with positive and negative charges were placed between the electrolyte solvent and the electrode, which was similar to a capacitor. The Helmholtz model was then modified by Goey and Chiman in 1910 and 1913, respectively. According to the model proposed by Gouy and Chapman, positive and negative ions were dispersed in the solvent (Fig. 1b). Finally, Stern combined the Gouy and Chapman model with the Helmholtz as shown in Fig. 1c. In Stern's model, ions with opposite charges are located in a region H.[73]

2.2. Pseudocapacitors

Pseudocapacitors were introduced to overcome the limitations of EDLC and mass transfer batteries. Pseudocapacitors have higher energy density than EDLCs due to the faradaic reaction.[40] Conducting polymers, TMO, TMS, and inorganic quantum dots

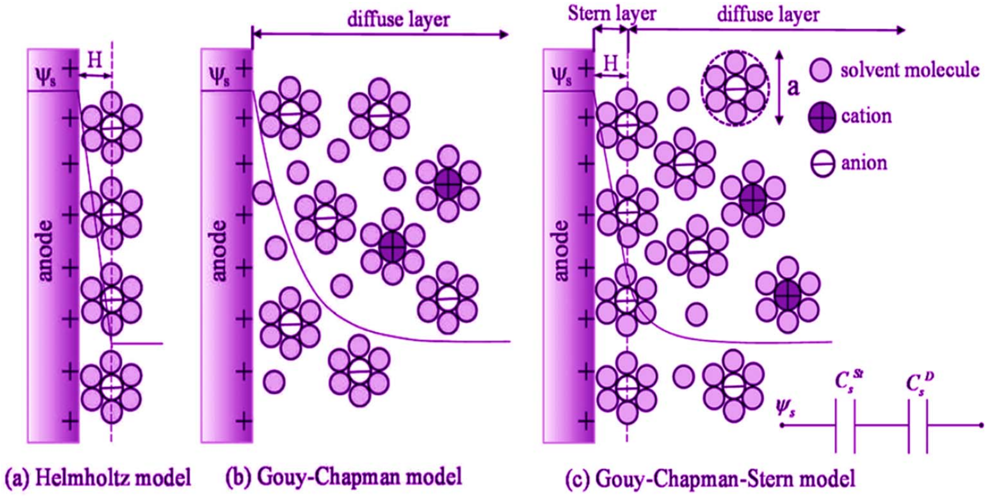

(a) Helmholtz model (b) Gouy-Chapman model (c) Gouy-Chapman-Stern model

Fig. 1 Schematic representations of EDL structures according to the Helmholtz model (a), the Gouy–Chapman model (b), and the Gouy–Chapman–Stern model (c). *H* is the double layer distance described by the Helmholtz model. C_s is the potential across the EDL.

were introduced as pseudocapacitors. However, pseudocapacitors as electrode material have limitations due to low power density and stability.[74]

2.3. Hybrid capacitors

Hybrid devices were developed to achieve an efficient supercapacitor with unique benefits. Hybrid capacitors were a combination of pseudocapacitor materials and EDLC materials, which are designed and manufactured in three main categories: the first category was composites, which include pseudocapacitor/EDLC composites.[75,76] The second category consisted of asymmetric devices made from pseudocapacitor materials and EDLC materials.[77] The third category is the battery type, which consists of a battery electrode and a supercapacitor electrode.[78,79]

3. Conductive polymers

Conducting polymers have the properties of conventional polymers and the conductivity of metals, simultaneously. Conductive polymers have high electrical conductivity due to the π-electron delocalization in conjugated backbones. The type of synthesis method affects the conductivity of these polymers.[80]

3.1. Polyacetylene

The first reports on polyacetylene (PA) were published in 1958–1970.[81] Polyacetylene (PA) has repeating units $(C_2H_2)_n$.[82] Polyacetylene was introduced as a semiconducting polymer. The conductivity of polyacetylene was investigated by Hideki Shirakawa, Alan MacDiarmid, and Alan Heeger, who received the Nobel Prize in 2000 for achieving these results. Heeger, MacDiarmid, and Shirakawa reported that the conductivity of polyacetylene increases with the addition of an oxidizing agent or a reducing agent.[83] The p-doped polymer was synthesized by adding an oxidizing agent (I2), and the n-doped polymer was synthesized by adding a reducing agent (sodium naphthalenide). The conductivity of polyacetylene increased by 11 orders with the addition of an oxidizing agent (I2). However, the stability of polyacetylene decreased with the addition of an oxidizing agent or a reducing agent. Therefore, the preparation of highly conductive and stable polyacetylene has been a challenge for researchers. In recent studies, various derivatives of polyacetylene have been synthesized by different methods.[84,85]

3.2. Polythiophene

Polythiophene is a conjugated polymer composed of repeating thiophene units. Polythiophene has unique properties that make it attractive for various applications such as supercapacitors,[86] sensors,[87,88] non-linear optics,[89] photoresists,[90] solar cells,[91] *etc.* Polythiophene has high heat resistance, making it suitable for industrial applications. Polythiophene is a soluble polymer with high conductivity; therefore, it has been investigated as an electrode material in many studies. The electrochemical performance of polythiophene can be controlled by doping. Numerous structural derivatives of this polymer have been reported with facile synthesis methods.[92] Liu *et al.* designed and synthesized various morphologies of polythiophene by oxidative polymerization. The morphology of polythiophene was investigated by controlling different synthesis conditions, including reducing agent concentration, catalyst concentration, and oxidizing agent concentration. The results showed that morphologies of spherical, filamentous, and ribbon were obtained by controlling different synthesis conditions.[93] Arvas *et al.* synthesized polythiophene with zigzag morphology using the electropolymerization method. Different dopants were used to modify the morphology of polythiophene, and the use of bromothymol blue dopant resulted in a zigzag morphology. The zigzag morphology increased the specific

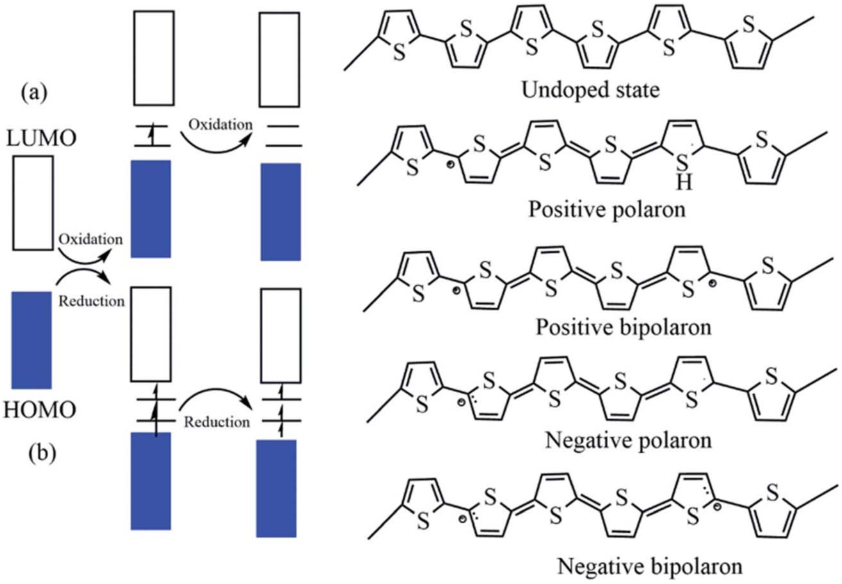

Fig. 2 The electronic band and chemical structures of polythiophene (PT) with (a) p-type doping and (b) n-type doping.

surface area of polythiophene. Polythiophene and zigzag polythiophene had specific surface areas of 32.629 $m^2 g^{-1}$ and 13.812 $m^2 g^{-1}$, respectively. The zigzag polythiophene electrode material showed a specific capacitance of 443.5 F g^{-1} at 5 mV s^{-1}. Polythiophenes exist in n-doped and p-doped forms. The specific and conductivity of polythiophene in n-doped form are lower than in p-doped form. Therefore, polythiophenes act as cathodes. N-doped polythiophenes have low stability in the presence of oxygen, so polythiophene derivatives were synthesized to overcome this limitation.[94] Undoped polythiophene acts as an insulator or semiconductor. Therefore, doped polythiophene acts as a conductive electrode material. Doped polythiophenes participate in oxidation and reduction reactions. Various dopings are performed on the polythiophene surface, including n-type doping, p-type doping, and polarons/bipolarons. These carriers delocalize the charge on the polythiophene chain, as shown in Fig. 2. In n- and p-type doping, electrons migrate from LUMO and HOMO to the polythiophene skeleton, respectively.[95]

3.3. Polyaniline

Polyaniline is the perfect electrode material for a supercapacitor, which is synthesized through chemical or electrochemical oxidation of aniline. Electrochemical polymerization works faster than chemical polymerization.[96] The electrochemical polymerization synthesis method was oxidant-free and environmentally friendly. Polyaniline exists in three states: reduced (leucoemeraldine), semi-oxidized (emeraldine), and oxidized (pernigraniline). The only electrically conductive form is the protonated form of the base of ameridine, the ameridine salt. The ameridine (E) protonated is produced using the oxidative polymerization of aniline in aqueous acids. Basic sites, including amine and imine in the polymer structure, facilitate protonation of ameridine in acidic solvents. Polyaniline exhibits various physical and chemical properties by applying a potential (−0.2 to +1.0 V). Polyaniline changes from pale yellow leucoemeraldine (L) to the green emeraldine salt/base (E) and finally to the purple pernigraniline form (P). Polyaniline obtained from these three oxidation states performs well in supercapacitor devices. The type of polyaniline synthesis method affects its final morphology. Polyaniline synthesized by electrochemical methods often has a granule-like morphology.[97] Polyaniline has shown excellent electrochemical properties, good stability, and ease of synthesis. Therefore, polyaniline has been widely used in the fabrication of supercapacitors. However, polyaniline has limitations such as conductivity variation, processing challenges, mechanical properties, sensitivity to dopants, and environmental contamination. Therefore, the optimal PANI can be determined by selecting the appropriate dopant, the amounts of aniline and oxidant monomer, and other preparation conditions (temperature and time).[98] Therefore, polyaniline/other electroactive material composites have been introduced as promising electrode materials. A successful method for improving the performance of polyaniline is to blend it with other polymers that have good mechanical properties. The use of PANI as a conductive filler in other polymers (matrices) has attracted attention due to improved processability and relatively good mechanical properties.[99] Polyaniline requires protons for charging and discharging. Therefore, polyaniline has high performance in an acidic electrolyte. The charge storage mechanism of polyaniline in the aqueous aluminum solution is shown in Fig. 3. First, protons from the acidic solution were adsorbed onto nitrogen, forming a positive charge on the polyaniline chain. Then, the anions in the solution were adsorbed onto the polymer to neutralize the positive charge. The diffusion and outflow of ions caused the charge storage in the polyaniline.[100]

3.4. Polypyrrole

Polypyrrole was used as a conductive polymer with environmental stability and high conductivity in energy storage systems

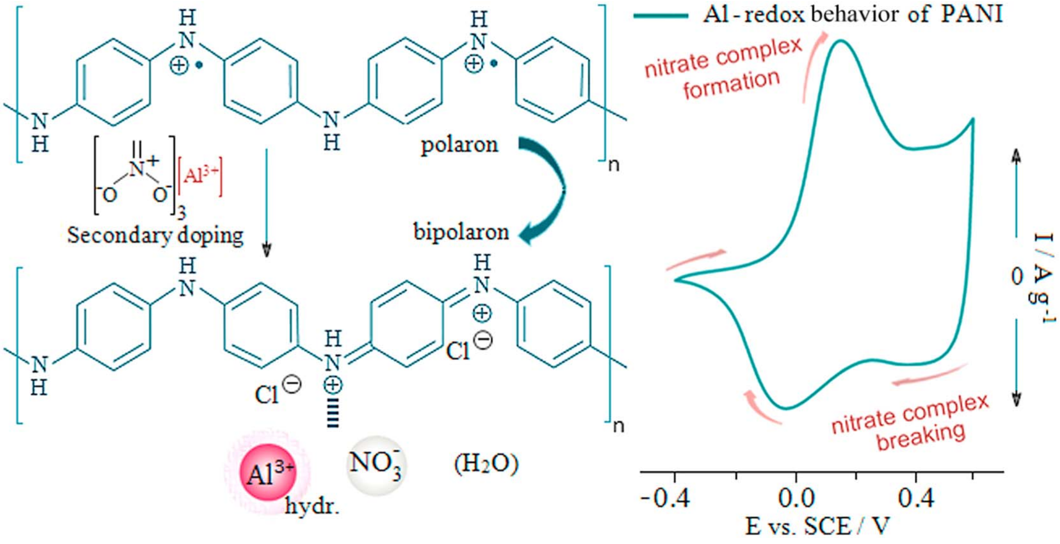

Fig. 3 Charge storage mechanism of polyaniline.

and various sensors.[101–103] Polypyrrole is a biocompatible heterocyclic polymer.[104] Polypyrrole exists as a conductive polymer with a positive charge in its oxidized form. Excessive oxidation of the nitrogen group reduces the polypyrrole's electroactive properties. Polypyrrole electrode materials have electroactive properties only in organic and aqueous solvents. Polypyrrole is synthesized using the polymerization of pyrrole units through various methods. The oldest method of polypyrrole synthesis is the oxidative polymerization of pyrrole in aqueous and organic solvents in the presence of oxidizing agents such as ammonium persulfate.[105,106] Polypyrrole synthesis methods include polymerization of photo, vapor phase, ultrasound, and microemulsion. The chemical oxidative method was used in industry despite numerous synthesis methods.[107,108] Unlike polythiophene, polypyrrole is not n-doped, so polypyrrole only acts as a cathode. Dense growth of polypyrrole limits access to internal sites of polypyrrole, thus reducing specific capacitance. The charge storage mechanism of polypyrrole occurs in several steps (Fig. 4). Undoped polypyrrole has low conductivity. When polypyrrole is doped with P-type materials, oxidation occurs, which converts the polypyrrole from benzoide to quinoid. Further oxidation accelerates the conversion of the benzoide form to quinoid due to the removal of the p-electron.[95]

3.5. Poly(3,4-ethylenedioxythiophene)

Poly(3,4-ethylenedioxythiophene) is known as a bioelectronic conductive polymer.[109] There are two different synthesis routes for poly(3,4-ethylenedioxythiophene). The first synthesis route is linear, multi-step, and lengthy, but the second synthesis route involves the addition of a thiophene ring, resulting in a shorter synthesis time; however, it is not economically viable. The advantages of poly(3,4-ethylenedioxythiophene), including optical transparency, biocompatibility, and conductivity, have led to numerous applications in solar cells,[110] glass,[111] light-emitting diodes,[112,113] textile fibers,[114] electroluminescence,[115] and cathode material in capacitors.[116,117]

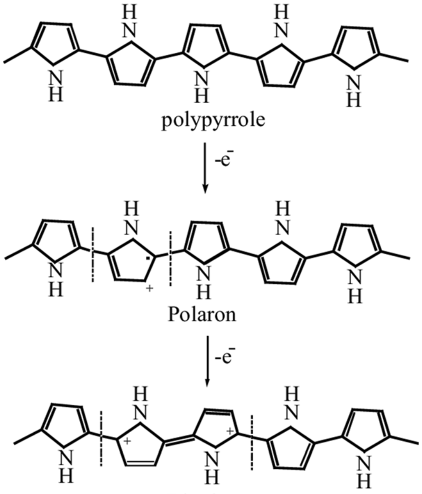

Fig. 4 Charge storage mechanism of polypyrrole.

3.6. Poly(phenylene vinylene)

Poly(phenylene vinylene) has luminescent properties and is a diamagnetic material with poor conductivity.[118,119] The conductivity of this polymer increases by doping with acids, sodium, potassium, and iodine. However, it has poor stability. Poly(phenylene vinylene) has numerous applications, including photovoltaics,[120,121] sensors,[122] and medical applications.[123,124]

3.7. Polyphenylene and polyparaphenylene

Poly(*para*-phenylene) is a linear polymer and has poor conductivity. This polymer can be made conductive by doping. Direct and pre-material methods for the synthesis of poly(*para*-phenylene) were reported.[125,126] The synthesis mechanism of the direct method is based on the Scholl method. The direct synthesis method results in powder form oligomers that are not processed. In the precursor method, poly(*para*-phenylene) derivatives are synthesized from soluble polymers. Microbial oxidative methods or chemical methods were used to synthesize precursors. For example, microbial oxidative benzene was used to prepare precursors for the synthesis of poly(*para*-phenylene).[127] In the chemical method, transition metal catalysts were used to prepare precursors, which had high yields but abundant impurities.[128] Chemical synthesis of precursors with *cis* and *trans* configurations was used to create poly(*para*-phenylene) for use in electronic devices.[129] The main application of poly(*para*-phenylene) has been in the aerospace and medical industries.[130,131]

4. The electrochemical energy-storage performance of composites based on CP

Conductive polymers such as PANI,[132] PPy,[133] and polythiophene derivatives have been recognized as effective high-performance electrode materials.[134] However, these electrode materials have limitations, including volume changes during repeated charging/discharging.[135] Other electroactive materials, such as various carbon materials (CNT, GO, rGO, CQD, and AC), MOF, and TMO or TMS have been used in supercapacitor systems. Conducting polymers or other electroactive materials alone have a limited role as electrode materials in supercapacitor systems. Therefore, by preparing two-component or multi-component composites of conducting polymers with other electroactive materials, efficient hybrid electrode materials can be achieved.[136,137]

4.1. The electrochemical energy-storage performance of carbon materials/CP composites

Carbon materials (CNT, GO, and AC) are electrode materials with EDLC behavior. Researchers synthesized composites of conductive polymers with other carbon materials to achieve efficient supercapacitor devices, which have high performance as hybrid electrode materials.

4.1.1. The CNT/CP composites for supercapacitors. CNTs were introduced as suitable electroactive materials due to their desirable properties for supercapacitor systems, including high conductivity, high specific surface area, and high stability. Carbon nanotubes (CNTs) are divided into two categories: single-walled carbon nanotubes (SWCNTs) and multi-walled carbon nanotubes (MWCNTs). However, the EDLC behavior of carbon nanotubes limits the achievement of electrode materials with desirable properties. Composites prepared from conductive polymers and carbon nanotubes showed more ideal supercapacitor properties. Qin *et al.* synthesized a core–shell morphology of polyaniline and CNT *via in situ* polymerization. The chemical analysis confirmed the formation of a 50 nm polyaniline layer on the carbon nanotube. Electrochemical analyses of the carbon nanotube and composite showed the synergistic effect of this core–shell structure, high stability, and specific surface area. Thus, electrode material of the core–shell showed 305 F g^{-1} at 1 A g^{-1}.[138] Liu *et al.* synthesized polyaniline/CNT composites by an innovative method. First, according to Fig. 5a, polyaniline dissolved in sulfuric acid was synthesized through several synthesis steps using acid chloride, aniline, and $(NH_4)_2S_2O_8$ precursors (polyaniline dissolved in sulfuric acid). In the second step, the carbon nanotube was immersed in a conductive solution (polyaniline dissolved in sulfuric acid). The sulfuric acid increases the contact surface between the polyaniline and the carbon nanotube. As the immersion time of the carbon nanotube in the conductive ink increased, the morphology changed to a shell structure, which increased the

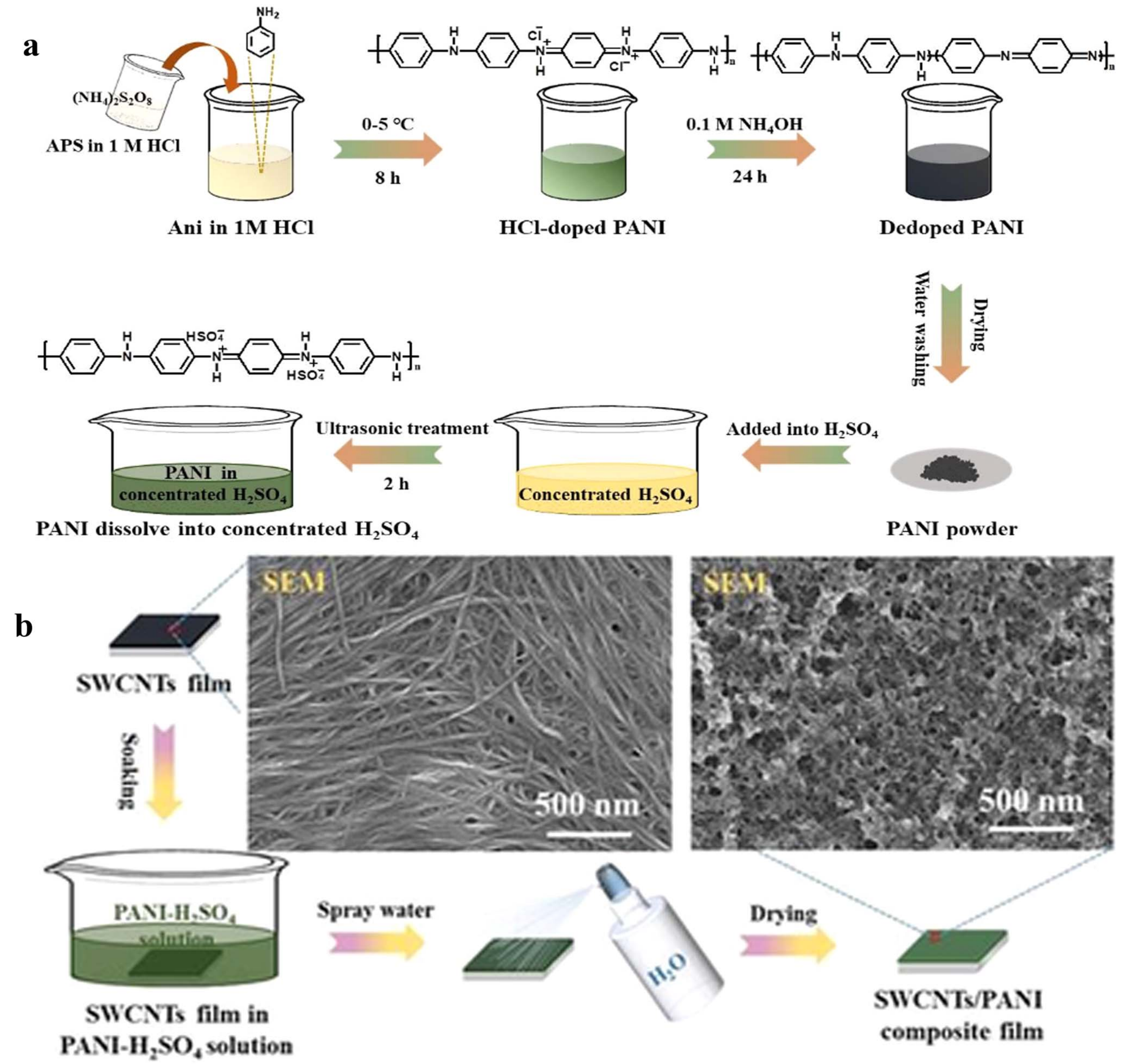

Fig. 5 (a) A general scheme for the preparation of PANI–H2SO4 solution and SWCNTs/PANI composite. (b) The SEM of SWCNTs/PANI and the SWCNTs film.

electrolyte penetration rate and increased conductivity. The results of the SEM analysis confirmed the shell structure with increasing immersion time (Fig. 5b). The composite of polyaniline/carbon nanotube showed 329 F g^{-1}.[139]

Polypyrrole demonstrated superior performance compared to polyaniline in composites of CNT and CP as an electrode material. The tubular structure of carbon nanotubes causes them to aggregate and limits their electrochemical performance. By converting MWCNTs into UzMWCNTs, the electrochemical properties are improved. In other words, by converting MWCNTs into UzMWCNTs, it is possible to achieve a higher specific surface area.[140,141] Therefore, UzMWCNTs are obtained by transverse and longitudinal modification of multi-walled nanotubes, and can simultaneously exhibit properties of graphene and nanotubes. There are various ways for synthesizing UzMWCNTs, including solid-state reaction, ball milling, electrochemical, *etc.*[142] Theresa *et al.* used the Hammer method to convert MWCNTs into UzMWCNTs. Then, a 5 wt% solution of UzMWCNTs was prepared and subjected to ultrasonic waves. PPy was mixed with the solution at 0 °C, and the composite of UzMWCNTs and polypyrrole was synthesized after 24 h of stirring. The highly conductive UzMWCNT/PPy hybrid electrode material showed 944 F g^{-1} at 1 A g^{-1}.[143] The morphology of polypyrrole and carbon nanotube-based composites affects their electrochemical behavior. Lin *et al.* synthesized polypyrrole/carbon nanotubes 3D composites with different morphologies using the electrodeposition method. Different nanocomposites were synthesized by varying the type of polypyrrole deposition method on carbon nanotubes. Polypyrrole with morphologies of nanoparticles, nanowires, and vertical nanowires was deposited on the nanotubes (Fig. 6). Electrochemical analysis was performed for three flexible supercapacitors prepared from these composites. The results confirmed the high conductivity of the flexible supercapacitor prepared from polypyrrole with vertical nanowire arrangement. PPy nanowire/CNTF provided a higher specific surface area than PPy nanoparticles/CNTF due to the wire morphology. The PPy VANA-/CNTF provided higher accessibility of electrolytic ions than the PPy nanowire/CNTF due to porous morphology. Therefore, the conductivity, specific capacitance, and coulombic efficiency of PPy VANA-/CNTF were higher than PPy nanowire/CNTF and PPy nanoparticles/CNTF. The flexible

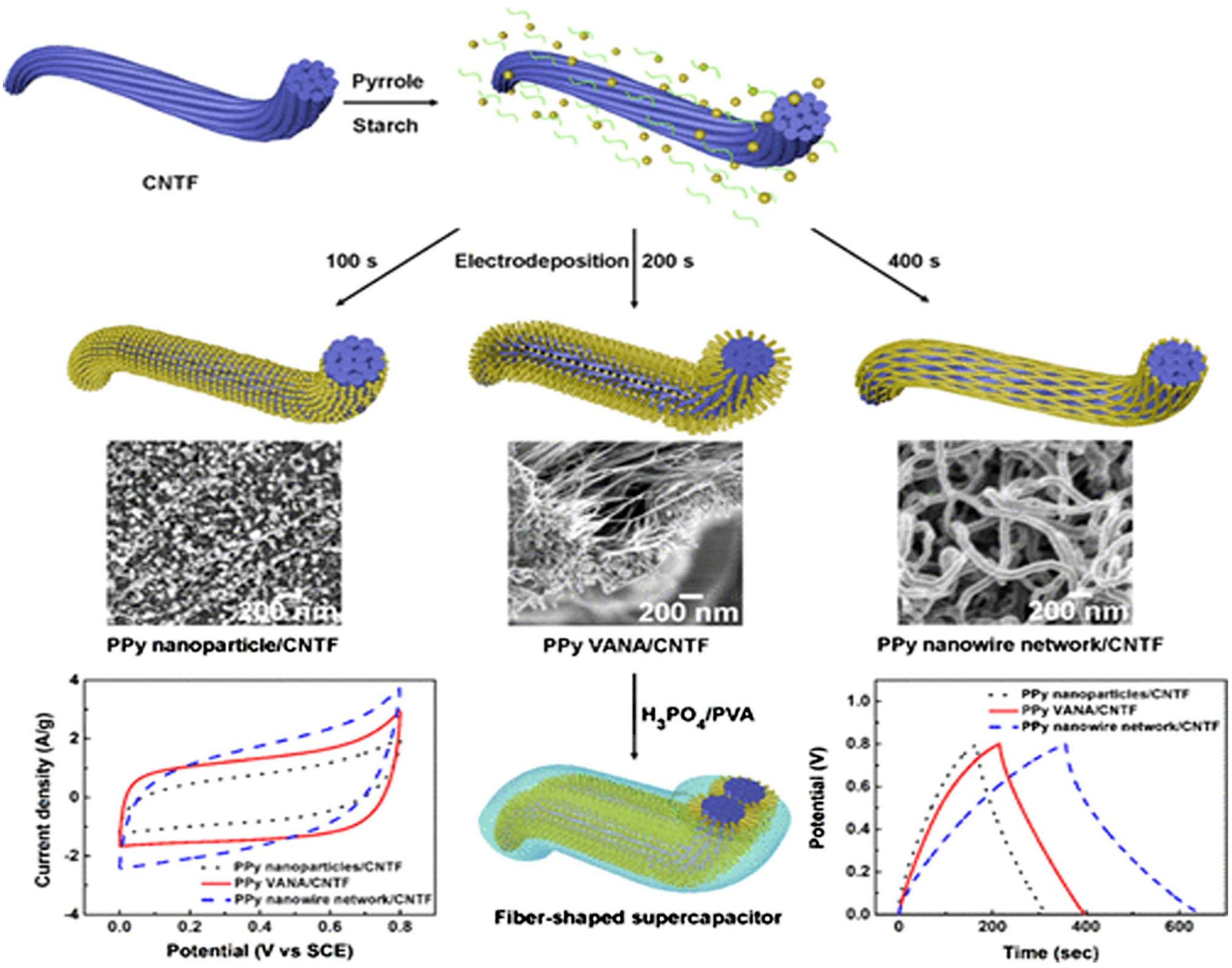

Fig. 6 A general scheme for the preparation of PPy VANA-/CNTF composite.

supercapacitor device prepared from the PPy VANA-/CNTF composite recorded the highest specific capacitance (178.14 F g^{-1} at 0.4 A g^{-1}).[144]

4.1.2. The GO/CP composites for supercapacitors. Graphene oxide is a two-dimensional material derived from graphene that has been used in energy storage systems as a conductive component in hybrid electrode materials. The hydroxyl and carboxyl functional groups in graphene oxide improve its hydrophilic properties. However, graphene oxide has a lower conductivity than graphene due to the disruption of the sp^2 bond network that occurs after oxidation and the formation of oxygen-containing functional groups. Therefore, composites of graphene oxide with other electroactive materials such as PANI, PPy, and polythiophene were designed and fabricated to achieve efficient electrode materials. Sharma *et al.* proposed a novel method for the synthesis of a two-dimensional composite of polythiophene and GO. A nano-reactor system (NRS) was used for the synthesis of the composite. This synthesis method aimed to preserve the two-dimensional morphology of graphene oxide during the synthesis of the composite and also facilitate the nucleophilic reaction. The rGO–PTs composite showed high specific capacity and high cyclic stability in HCl electrolyte.[145] Ates *et al.* synthesized two composites using the chemical electrospinning method to compare the effect of GO and rGO on improving the electrochemical performance of polythiophene-based composites. Electrochemical analyses confirmed the high capacitance and conductivity of the composite containing rGO. Then, the performance of rGO/PTh/CB and rGO/CB was compared. Corresponding to the results of electrochemical analyses, the specific capacitance increased by 6 times in the presence of polythiophene.[146] In another study, N–N-doped rGO was used to synthesize the composite. The Pth/n-rGO composite was synthesized *via* the polymerization and showed 455 F g^{-1} at 1 A g^{-1}.[147] Composites of PANI and rGO have been reported in recent studies to achieve an efficient electrode mode. Polyaniline prevents the aggregation of graphene oxide and increases the specific surface area. Polyaniline increases the active sites for the reaction. Reduced graphene oxide increases the electron transfer rate. Therefore, the rGO@PANI composite electrode material was identified as an efficient electroactive material. Umar *et al.* prepared the rGO@PANI by a facile method, and the results showed 314.2 F g^{-1} at 1 A g^{-1}.[148] Arumugam *et al.* first synthesized GO through the method of the Hammer, then synthesized a GO/PANI composite through the *in situ* polymerization method. The electrochemical results recorded the achievement 255 F g^{-1} at 10 A g^{-1}.[149] In addition to polythiophene and polyaniline, the supercapacitor behavior of polypyrrole/GO composites has also been reported in recent studies. Suranshe *et al.* prepared PPy/GO composite *via* the electrochemical method. First, GO was synthesized *via* electrochemical exfoliation of graphite rods, and then the composite was prepared through method of the electrochemical. The results showed the synergistic effect between GO and polypyrrole.[150]

4.1.3. The GO/CP/CNT composites for supercapacitors. Three-component composites (graphene/carbon nanotube/conductive polymer) were designed and synthesized to achieve specific surface area and higher conductivity.[151,152] Zhang *et al.* synthesized a PANI/G/carbon nanotube by *in situ* polymerization. First, aniline and ethanol were added to a $HClO_4$ solution. Then, graphene was mixed with the resulting solution in the oxidizing agent at low temperature, and carbon nanotubes were added to the solution. After 24 hours, the composite was synthesized. The composite was placed on a polyurethane film. Composites were synthesized with different graphene ratios (CGP-1, CGP-1.5, CGP-2). The results of electrochemical studies showed that increasing the graphene ratio (from CGP-1 to CGP-1.5) improved the conductivity and specific capacitance. An increase in the graphene ratio (CGP-2) disrupted the ion diffusion process and increased charge transfer resistance. The CGP-1.5 electrode was a flexible electrode that retained 80% of its capacity after tensile testing for 10 cycles.[153] Albdiry *et al.* synthesized the sulfonated graphene/PANI/CNT composite *via* a two-step. The first step involved *in situ* mixing, and the second step involved dispersion. Sulfonation of graphene increased the distance between particles, which prevented the expansion of polyaniline chains. Sulfonation of graphene increased the electrolyte penetration rate in the ternary composite.[154] Aphale *et al.* synthesized graphene/carbon nanotubes/polypyrrole hybrid electrode materials by *in situ* polymerization. The electrochemical behavior of polypyrrole and polypyrrole/graphene/CNT composites was investigated to examine the effect of graphene and carbon nanotubes on improving the electrochemical behavior. First, the electrochemical behavior of the polypyrrole and polypyrrole/graphene/CNT composites in the electrolytes of sulfuric acid, sodium sulfate, and ascorbic acid was investigated. The results of electrochemical analyses showed that both electrode materials had better electrochemical performance in the presence of sulfuric acid electrolyte. The polypyrrole electrode materials and the polypyrrole/graphene/CNT composites electrode materials showed specific capacitances of 281 F g^{-1} and 305 F g^{-1}, respectively. Finally, the specific capacitance increased to 453 F g^{-1} with increasing concentrations of graphene and CNT.[155] In another study, hybrid GN/AC was synthesized using vacuum filtration, and then an electrochemical process was used for electrodeposition of polypyrrole. First, electrodeposition was performed at areal current density of 5, 10, 15, and 20 mA cm^{-2} for 200 seconds. Then, electrodeposition was performed at 100, 200, and 300 seconds in a areal current density of 15 mA cm^{-2}. The GN/AC/PPy15-200 s electrode material recorded a maximum specific capacitance of 178 F g^{-1} at 0.5 A g^{-1}.[156]

4.1.5. The CQD/CP composites for supercapacitors. Carbon quantum dots (CQDs) are a class of zero-dimensional materials that have good solubility, low toxicity, porosity, and efficient charge transport. Therefore, they have many applications in medicine,[157,158] sensors,[159] catalysts,[160] and energy storage devices. In general, carbon quantum dots cause dispersion and porosity in conductive polymers, thereby increasing conductivity. Devendrappa *et al.* synthesized water-soluble quantum dots by the hydrothermal method, then synthesized polypyrrole/CQD by the *in situ* polymerization method. The morphology of polypyrrole was controlled by preparing composites with different ratios of carbon quantum dots. The composite with the optimal ratio showed 750 F g^{-1} at 1 A g^{-1}.[161] Liu *et al.* grew rare CQD on cotton fabric, then pyrrole was grown *via in situ* polymerization. The composite electrode material was introduced as an efficient system in smart textiles. The CC@CQD@PPy shows 537.9 F g^{-1} at 0.5 A g^{-1}.[162] Chen *et al.* synthesized the composite of PANI and CQD through oxidative polymerization. An asymmetric system of polyaniline/carbon quantum dots and V_2O_5@PEDOT was designed and fabricated (Fig. 7). The asymmetric device exhibited high energy density, high dyeing efficiency, and high stability.[163]

Mehare *et al.* synthesized CQD derived from sucrose with different sucrose ratios (10, 15, 25, 30). Then, the composite based on polyaniline and CQD was synthesized through the electrodeposition. According to electrochemical analyses, the composite synthesized from carbon quantum dots with a ratio of 25 has high specific capacitance, high stability, and lower resistance.[164] Zhang *et al.* designed a polyaniline/carbon-based quantum dots/carbon nanofibers electrode using a hierarchical method. The 3D structure of this electrode accelerated the movement of ions. According to the analysis results of electrochemical and chemical, the functional groups of carbon quantum dots increased conductivity by creating multiple active sites for charge transfer.[165] Yıldız *et al.* synthesized the PANI/N-doped CQD composite through *in situ* polymerization. Investigation of the electrochemical behavior of the composite, PANI, and N-doped CQD confirmed that the electrolyte transfer rate in the composite was improved compared to polyaniline and N-doped CQD. The composite electrode material exhibited 503 F g^{-1} (5 A g^{-1}) and 91.9% (10 000 cycles), respectively.[166] Duraisamy *et al.* used poly(aniline-*co*-indole) to prepare a composite based on CP and CQD (hybrid electrospray synthesis method). The asymmetric supercapacitor of poly(aniline-*co*-indole)/CQD and rGO recorded 26.22 W h kg^{-1}. According to the standard Ragone plot of supercapacitors, the standard energy density of supercapacitors is 0.1–100 W h kg^{-1}. The reported energy density of asymmetric devices with CQD-based electrodes is 26.22 W h kg^{-1}, which corresponds to the standard Ragone plot of supercapacitors (Table 1).[167]

4.2. The electrochemical energy-storage performance of metal oxide or sulfide/conductive polymers composites

Metal oxides or sulfides have higher energy density than carbon materials.[183] TMO or TMS have low conductivity, limited specific surface area, and low stability. Therefore, to achieve efficient electroactive materials, ternary composites of CP, TMO (or TMS), and C have been synthesized. However, bimetallic oxides and sulfides have higher redox potential, higher conductivity, and stability than monometallic oxides and sulfides. Therefore, binary composites of bimetallic oxides or sulfides and conductive polymers perform well as electroactive materials. Preparing binary composites of CP and bimetallic oxides or sulfides as electroactive material is a more economical and industrially feasible method than ternary composites of CP, C, and TMS (or TMO). Shehzad *et al.* synthesized composites based on conductive polymer (PANI) and $NiCo_2O_4$ by hydrothermal method. The synergistic effect of polyaniline and $NiCo_2O_4$ resulted in increased conductivity and stability over cycles. The PANI/$NiCo_2O_4$ electrode material maintained 100% stability after 5000 cycles.[184] Shanmugavalli *et al.* synthesized $NiCo_2O_4$ and $NiCo_2O_4$/PANI by solution combustion and physical blending methods, respectively, to achieve a cost-effective synthesis method. According to chemical analyses, the morphology of $NiCo_2O_4$/PANI provided special surfaces for electron transport. According to the results of electrochemical analysis of $NiCo_2O_4$ and $NiCo_2O_4$/PANI, the specific capacitance doubled with the addition of polyaniline (the specific capacitance of $NiCo_2O_4$/PANI was twice that of $NiCo_2O_4$).[185] Xue *et al.* first synthesized polyaniline using the *in situ* polymerization method, then designed and synthesized $NiCo_2O_4$/polyaniline

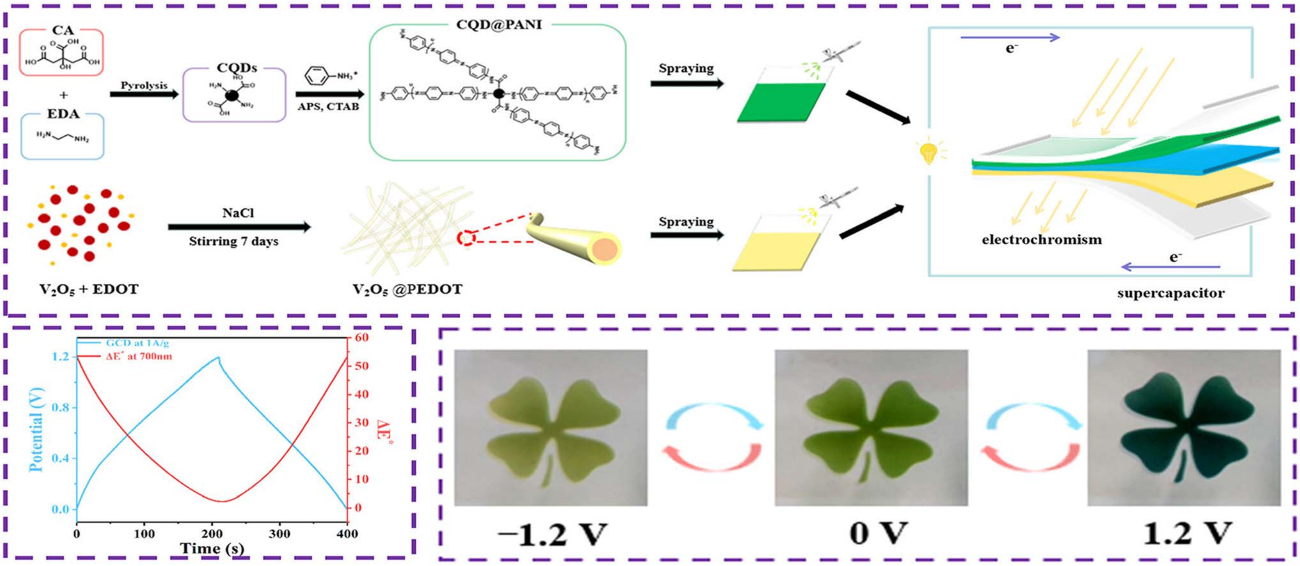

Fig. 7 A general scheme for the preparation of V_2O_5@PEDOT composite.

Table 1 The electrochemical data of C/CP composites

Sample	Stability (cycles)	Specific capacitance (or areal specific capacitance)	Current density (or areal current density)	Reference
Polyaniline/single-wall carbon nanotube (SWCNTs)	99% up to 1000	463 F g^{-1}	10 mA cm^{-1}	168
CNT/polyaniline	91% up to 1000	347 F g^{-1}	1.7 A g^{-1}	169
Ti_3C_2 MXene/PANI	90% up to 10 000	377 F g^{-1}	1 A g^{-1}	170
Multi-walled carbon nanotubes (MWCNTs)/PANI	—	248 F g^{-1}	0.5 A g^{-1}	171
GNPLs/PTh	84.9% up to 1500	673 F g^{-1}	0.25 A g^{-1}	172
Poly(3-hexylthiophene) (P_3HT)/SWCNTs	80.5% up to 1000	245.8 F g^{-1}	0.5 A g^{-1}	173
Polythiophene (PTP)–CNT	—	125 F g^{-1}	1 A g^{-1}	174
Graphene oxide–polythiophene derivative hybrid nanosheet	91.86% up to 4000	296 F g^{-1}	0.3 A g^{-1}	175
PPy/CNT	95% up to 5000	211 F g^{-1}	0.2 A g^{-1}	176
Graphene/Polythiophene	94.5% up to 1500	365 F g^{-1}	1 A g^{-1}	177
GO@PPy	90% up to 1000	1532 mF cm^{-1}	0.88 mA cm^{-1}	178
GO@PPy	76% up to 6000	0.23 F cm^{-1}	1 mV s^{-1}	179
N-CQD/PANI	74.7% up to 2000	498 F g^{-1}	1 A g^{-1}	180
CQDs/PPy	85.7% up to 2000	308 F g^{-1}	1 A g^{-1}	181
CQDs–PANI	78.0% up to 1000	738.3 F g^{-1}	1 A g^{-1}	182

composite on nickel foam using the hydrothermal method. Electrochemical analysis showed the synergistic effect of polyaniline and $NiCo_2O_4$. The composite electrode material based on $NiCo_2O_4$ and polyaniline recorded 3108 F g^{-1} at areal current density 1 mA cm^{-2}.[186] Nandi *et al.* synthesized composites of polythiophene and $NiCo_2O_4$ with different ratios (1–1 and 1–2) by the oxidative polymerization method. The results of the chemical analysis showed the porous matrix of polythiophene on $NiCo_2O_4$. According to electrochemical analysis, the $NiCo_2O_4$/polythiophene composite with a ratio of 1–1 had higher stability than the ratio of 1–2.[187] In another study, composites based on polyaniline and $NiFe_2O_4$ with different ratios were synthesized through the *in situ* polymerization. However, by changing the type of metal oxide, the $NiFe_2O_4$/polyaniline composite with a ratio of 2–1 had more optimal supercapacitive behavior as an electroactive material.[188] The composite of polyaniline and $MnCo_2O_4$ synthesized by polymerization showed 185 F g^{-1}.[189] Sui *et al.* synthesized core–shell structures based on polyaniline and $MnCo_2O_4$ by two synthesis steps: electrodeposition and hydrothermal. The conductivity resulting from polyaniline and the high specific surface area of $MnCo_2O_4$ led to the achievement of electrode materials with a specific capacitance of 1098 F g^{-1} at 1 A g^{-1}.[190] Varma *et al.* designed and synthesized composites based on $MnCO_2O_4$ and polyaniline with different proportions of polyaniline (0–30%) by the co-precipitation. The electrochemical analyses showed the composite with a 20% polyaniline ratio as the optimal ratio (high conductivity and stability). The optimal composite ratio (20%) showed a specific capacitance of 765 F g^{-1} at a current density of 0.5 A g^{-1}.[191] Chen *et al.* grew a composite based on polyaniline and $NiCo_2O_4$ on carbon tissue in three synthesis steps as shown in Fig. 8. The results of electrochemical analyses for the composite and composite components confirmed the synergistic and enhancing effect of polyaniline. The $NiCo_2O_4$/PANI electrode material showed a maximum stability of 99.64% over 10 000 cycles.[192]

Merlin *et al.* designed and synthesized a nanocomposite of polyaniline and $CuCo_2O_4$ as a quasi-capacitor electrode material, which was synthesized through an *in situ* polymerization method. Electrochemical analyses of the nanocomposite and polyaniline confirmed the increase in specific capacitance and conductivity with the addition of polyaniline. In other words,

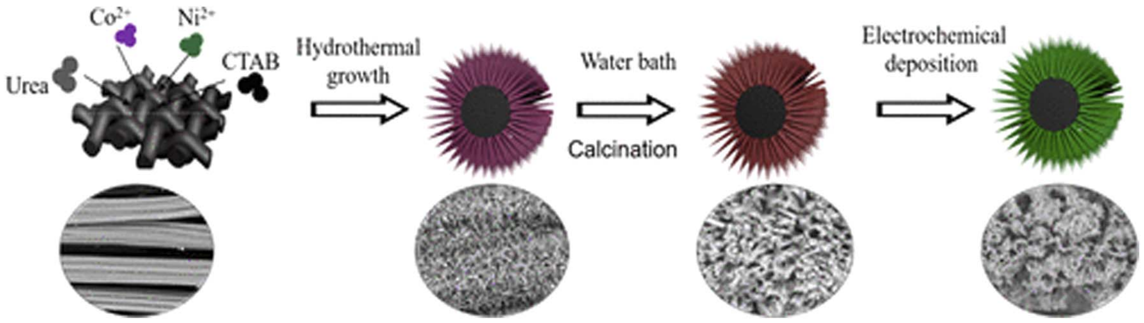

Fig. 8 A general scheme for the preparation of $NiCo_2O_4$/PANI composite.

the active sites for ion transport increased, and the synergistic effect led to the achievement of an efficient electrode material with stability of 98.5% after 5000 cycles.[193] The $CuCo_2O_4$ electrode materials have low permeability and low stability, which can be improved by compositing with conductive polymers. In recent studies, the preparation of polypyrrole/$CuCo_2O_4$ as electroactive materials was reported to achieve efficient electrode materials with high specific capacity and stability. The $CuCo_2O_4$/polypyrrole composite electrode showed 912 F g^{-1} at 2 A g^{-1}.[194] Chen *et al.* synthesized a composite based on polyaniline and $ZnCo_2O_4$ using zinc nitrate, cobalt nitrate, and NH_4F precursors using two steps (hydrothermal and *in situ* polymerization). The asymmetric device of polyaniline/$ZnCo_2O_4$ composite and AC showed 66.6 W h kg^{-1}.[195] Benyoucef *et al.* synthesized polyaniline/CuO/ZnO/MnO by the co-precipitation method. The high specific surface area of polyaniline/CuO/ZnO/MnO was confirmed by chemical analysis. Therefore, this composite showed the specific capacitance of 451.4 F g^{-1} at 5.0 mV s^{-1} in potassium hydroxide electrolyte solution due to high stability and short electron transport path.[196] Iqbal *et al.* also synthesized ternary, quaternary, and monolayer composites of polyaniline, Pr_2O, NiO, and Co_3O_4 through the co-precipitation method. The specific capacitance of the quartet composite (PANI–NiO, PANI–Co_3O_4) was twice that of the ternary composite (Pr_2O_3–NiO–Co_3O_4) and four times that of the binary composites.[197] In addition to composites based on bimetallic oxides and conductive polymers, other studies of composite electrode materials based on monometallic oxides and polymers were reported. For example, Shim *et al.* grew polyaniline/3D CoO on nickel foam by the electrochemical polymerization, which recorded a 2473 F g^{-1} at 3 A g^{-1}.[198] Metal sulfides or bimetallic sulfides are high-performance quasi-capacitor materials that have better electrochemical behavior than TMO. Sulfur is less electronegative than oxygen, so metal sulfides have excellent electrochemical behavior in conductive composites of CP. Li *et al.* synthesized a composite of PPy (prepared in an ice bath) and nickel–cobalt bimetallic sulfide through *in situ* polymerization in two steps. According to the results of chemical analyses, the use of the *in situ* polymerization synthesis method resulted in homogeneous synthesis of

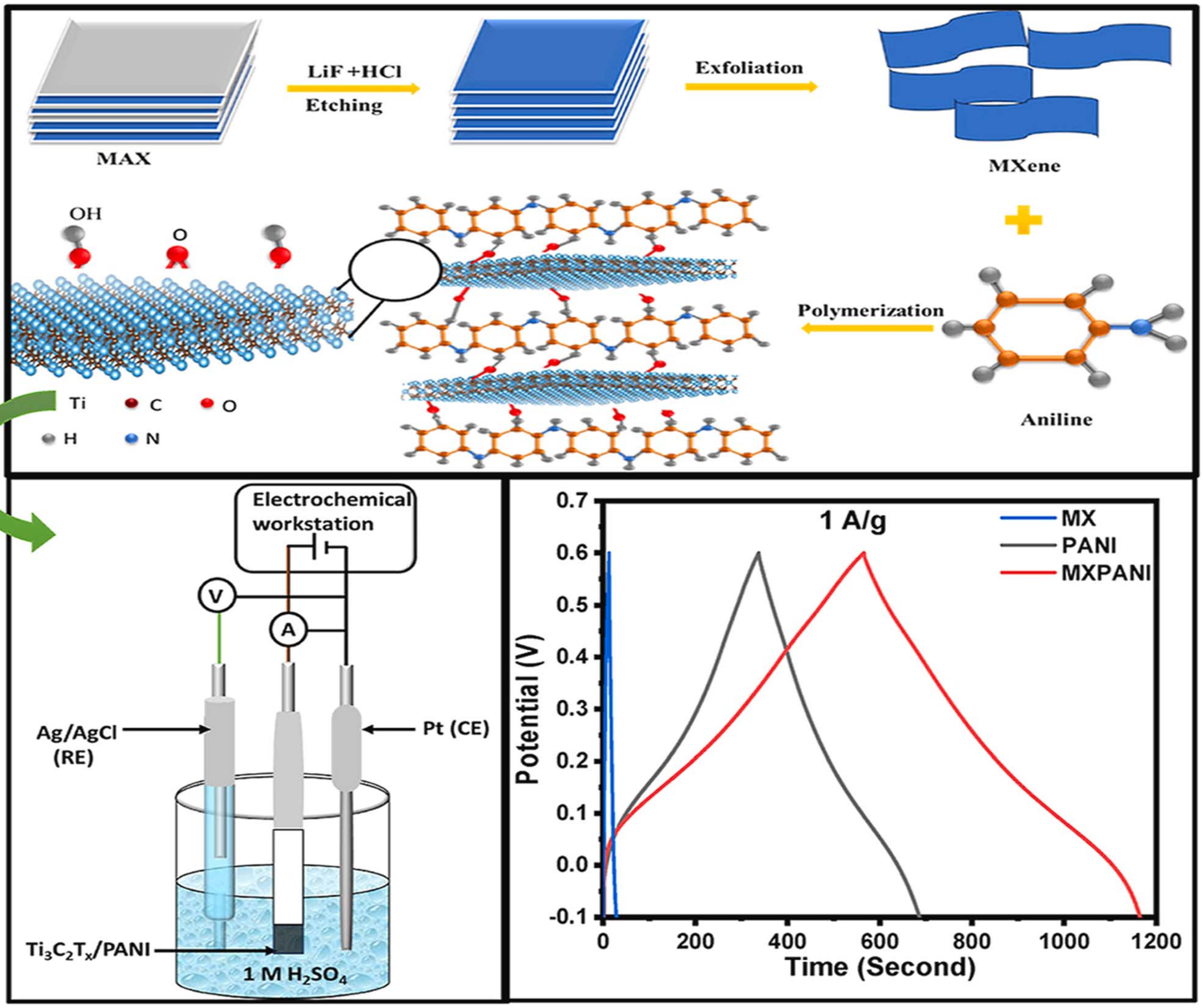

Fig. 9 A general scheme for the preparation of PANI/FeS_2/MnO composite.

the composite, thus increasing the contact between the electrolyte and the composite electrode materials. The asymmetric device of NiCo bi-metal sulfide/polypyrrole composite and AC recorded 44.5 W h kg^{-1}.[199] The ammonium ion supercapacitor has high efficiency due to reduced environmental pollution. However, it has limitations that can be overcome by choosing appropriate. The ammonium ion has a low capacitance contribution at the electrode surface compared to common ions such as lithium. A composite based on MoS_2 and polyaniline was used to prepare an ammonium ion supercapacitor, which showed 450 F g^{-1}.[200] Ulaganathan *et al.* synthesized electrode materials of MoS_2 and polyaniline with different weight ratios of MoS_2. Investigation of the electrochemical behavior of the composite in hydrogel electrolyte confirmed the optimal performance with a weight content of MoS_2 (5 wt%).[201] The musk structure is created by designing and synthesizing composites of TMS, TMO, and CP, which shortens the electron transport path and reduces the contraction and expansion of the polymer chain during charging/discharging. Yang *et al.* synthesized the MnO_2/polyaniline in two steps *via* oxidative polymerization (Fig. 9). By preparing different ratios of the ternary composite, the ratio PANI (4)/FeS_2 (1)/MnO (3) had higher stability.[202]

Bimetallic sulfides have more favorable electrochemical behavior than monometallic sulfides due to the synergistic effect of two transition metals. Qin *et al.* synthesized a hybrid based on NiMoS and polyaniline nanotubes by a hydrothermal chemical method, which was grown on polyaniline nanosheets. The increased conductivity of the polyaniline nanotubes and the numerous active sites created by NiMoS led to the achievement of an electroactive layer with 1558 F g^{-1} at 1 A g^{-1}.[203] In another work, electrode materials based on polypyrrole and $CuCo_2S_4$ were synthesized on nickel foil. According to chemical and electrochemical analyses, the oxidation states of copper and cobalt increased during charge–discharge, thus recording 1403.21 C g^{-1} at 1 A g^{-1} (Table 2).[204]

4.3. The electrochemical energy-storage performance of metal oxide or sulfide/conductive polymers/carbon materials or MXene composites

Composites of CP and TMO or TMS have low conductivity as quasi-capacitor electrode materials. Therefore, the conductivity is improved by adding carbon materials such as GO, AC, and CQD to composites based on CP and TMO.[232] Carbon materials increase the specific surface area and provide active sites for an energy storage system. Innovatively, Jia and colleagues synthesized polyaniline-based carbon through carbonization, then prepared a composite of cobalt oxide/polymer-based carbon. The composite electrode material was self-standing, which enabled its industrial application (no slurry preparation required).[233] The addition of graphene oxide to metal sulfide-conducting polymer or metal oxide-conducting polymer composites increases mechanical strength. However, metal oxides or sulfides improve the crystal structure. The composite prepared from polyaniline and GO as electrode material in the

Table 2 The electrochemical data of TMO/CP or TMS/CP composites

Sample	Stability (cycles)	Specific capacitance (or areal specific capacitance)	Current density (or areal current density)	Reference
$NiCo_2O_4$/PANI	86.2% up to 3000	561.2 F g^{-1}	10 mV s^{-1}	205
$NiFe_2O_4$/PANI	93.5% up to 7000	334 F g^{-1}	1 mA cm^{-2}	206
$CuMn_2O_4$/PANI	95% up to 7000	1181 F g^{-1}	1 A g^{-1}	207
Polypyrrole/$CuCo_2S_4$	90% up to 5000	259 F g^{-1}	1 A g^{-1}	208
$ZnBi_2O_4$/PANI	—	1110.12 F g^{-1}	1 A g^{-1}	209
CuO/PANI	75% up to 2000	185 F g^{-1}	1 A g^{-1}	210
PANI–Co_3O_4	84.9% up to 2000	1184 F g^{-1}	1.25 A g^{-1}	211
PANI–Co_3O_4	74.81% up to 3000	3105.46 F g^{-1}	1 A g^{-1}	212
$CuCo_2O_4$–PANI	94%% up to 3000	403 C g^{-1}	1 A g^{-1}	213
Co_3O_4/PANI	90%% up to 2000	1301 F g^{-1}	1 A g^{-1}	214
$FeCo_2O_4$/PANI	94.5% up to 5000	940 C g^{-1}	1 A g^{-1}	215
PANI/Fe–Ni codoped Co_3O_4	84%% up to 2000	1171 F g^{-1}	1 A g^{-1}	216
α-$MnMoO_4$/PANI	84% up to 2000	396 F g^{-1}	5 mV s^{-1}	217
MnO_2/PANI	95% up to 2000	687 F g^{-1}	5 mV s^{-1}	218
α-MnO_2/PANI	Excellent cyclic stability	696.66 F g^{-1}	0.5 A g^{-1}	219
Cerium oxide/PANI	90% up to 1000	950 mF cm^{-2}	10 mA cm^{-1}	220
$BaNiO_2$/PANI	97.9% up to 4000	1631 F g^{-1}	1 A g^{-1}	221
$CuCo_2S_4$/PANI	80.75% up to 3000	209 F g^{-1}	5 mV s^{-1}	222
$CuAlO_2$/PANI	—	1119.79 F g^{-1}	1 A g^{-1}	223
SnO_2/PANI	99.71% up to 5000	338 F g^{-1}	0.1 A g^{-1}	224
PANI/$CeVO_4$	90% up to 2000	1048 F g^{-1}	10 mV s^{-1}	225
MoS_2/PPY	75.7% up to 3000	677 F g^{-1}	1 A g^{-1}	226
PANI/PbS	95.5% up to 5000	625 F g^{-1}	1 A g^{-1}	227
MoS_2/PANI	89% up to 2000	645 F g^{-1}	0.5 A g^{-1}	228
polyaniline/MoS_2–MnO_2	94.1% up to 4000	479 F g^{-1}	5 mV s^{-1}	229
NiMnS–PANI	98% up to 10 000	976 C g^{-1}	7 A g^{-1}	230
PPy/PANI/MnO_2	84% up to 2500	136.64 F g^{-1}	2 A g^{-1}	231

study by Rani *et al.* showed 4800 F g^{-1} at 1 A g^{-1}.[54] Polyaniline caused uniform growth of nickel sulfide (preventing aggregation) in the synthesis of the nickel sulfide/polyaniline/graphene composite. Chang *et al.* investigated the electrochemical behavior of nickel sulfide/polyaniline/graphene composite. According to analyses of chemical and electrochemical, polyaniline caused uniform growth of nickel sulfide (preventing aggregation) in the synthesis of NiS_2/G/PANI composite. Graphene in the NiS_2/G/PANI composite structure increased the conductivity.[234] Acidic groups of graphene oxide sometimes act as dopants instead of HCL. Thus, preventing corrosion of metal sulfide in the composites based on PANI, TMS, and GO. Batabyal *et al.* synthesized a composite of MgS, GO and, PANI using HCL as a dopant. The uniform morphology of the MnS/GO/PANI composite improved the electrolyte diffusion rate, and graphene oxide improved the electrical conductivity.[235] Vadivel *et al.* synthesized a composite of $FeNiS_2$, CNT, and polypyrrole in a two-step synthesis process. The CNT in the composite structure acted as a support for polypyrrole, so the PPy/CNT/$FeNiS_2$ composite as a heterogeneous structure showed superior electrochemical performance with a 1541 F g^{-1} at 2 A g^{-1}.[236] Naeem *et al.* synthesized composites based of $NiCoFe_2O_4$, rGO and polypyrrole, using different ratios of nickel and cobalt. First, composites based on $NiCoFe_2O_4$ and rGO were synthesized through chemical combustion. Finally, the ternary composite was synthesized by adding polypyrrole through chemical oxidation. The optimal ratio of nickel to cobalt, along with the synergistic effect of the ternary composite, resulted 585 F g^{-1}.[237] Kiani *et al.* designed and synthesized an asymmetric device made of positive and negative electrodes. The negative electrode was a composite based on polypyrrole and titanium dioxide on carbon fabric by electrochemical deposition. Then it was plunged into the MXene solution in several steps. To prepare the positive electrode, the carbon fabric was immersed in sulfuric acid, nitric acid, and $KMnO_4$ solution. The electrochemical behavior of the negative electrode was investigated by several steps of immersion in MXene solution (Fig. 10). The asymmetric device showed 87% stability after 13 000 cycles.[238]

Jiang *et al.* prepared a core–shell structure based on polypyrrole, MnO_2, Fe_3O_4 in layered structures of graphene oxide using an industrial and cost-effective method. The four-component composite with a three-dimensional structure provided a high specific surface area for electron transport. The combination of two different metal oxides produced a high faradaic property. The synergistic effect of metal oxides with graphene oxide resulted in high-performance electrode materials.[239] Shaheen *et al.* synthesized AgNiO/rGO/PANI composite using a simple hydrothermal method. The synergistic effect and high specific surface area led to 1375.55 F g^{-1} at 0.5 A g^{-1}.[240] Composites of carbon materials, conductive polymer, and TMO with different percentages of conductive polymer were synthesized and investigated to achieve efficient electrode materials.

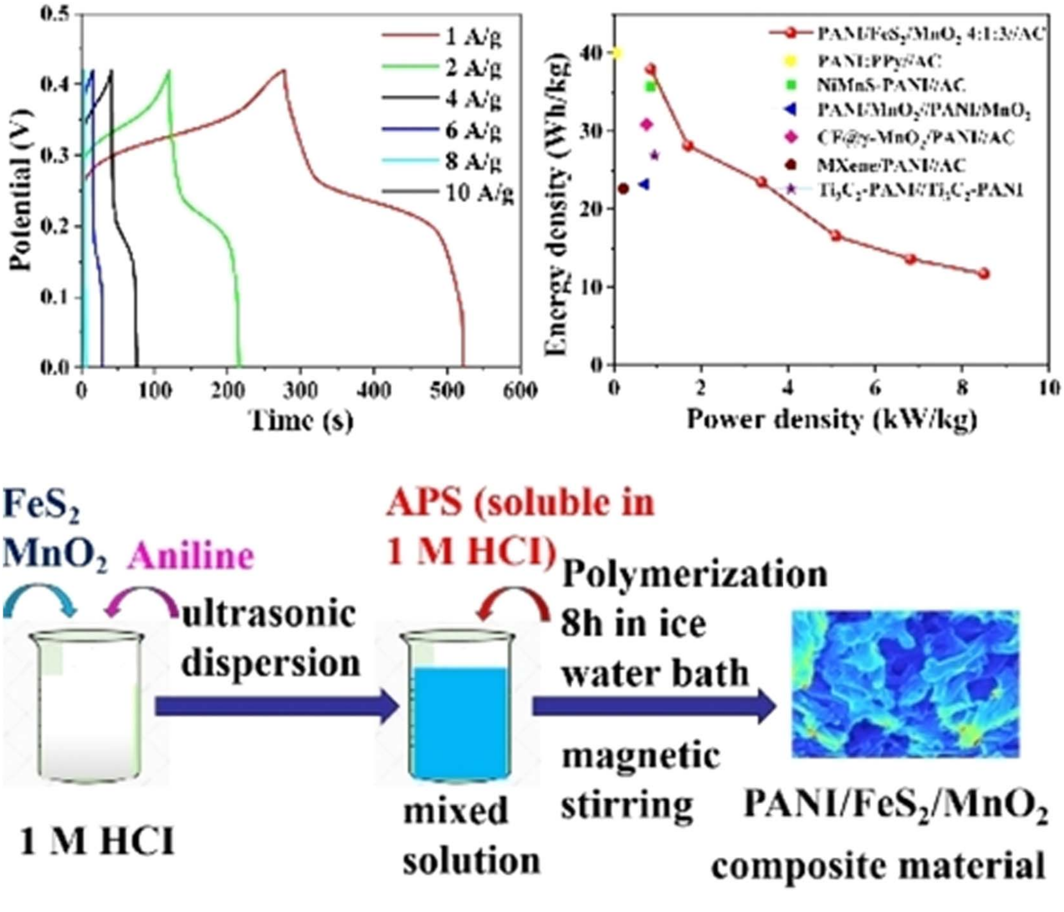

Fig. 10 A general scheme for the preparation of $Ti_3C_2T_x$/polyaniline composite.

Subbramaniyan *et al.* synthesized a quaternary hybrid of GO, MnO_2, MoO_3, and different ratios of polyaniline. The composite with the optimal ratio of polyaniline showed 596 F g^{-1} at 1 A g^{-1}.[241] Atram *et al.* synthesized the carbon nanofibers/$NiFe_2S_4$/polyaniline composite in two steps. First, a hybrid based on carbon nanofibers and $NiFe_2S_4$ was synthesized using electrospinning, and then polyaniline was added by *in situ* polymerization. The synergistic effect of the pseudocapacitor materials ($NiFe_2S_4$/PANI) and the EDLC materials (CNF) improved the supercapacitor performance, and the electrode materials showed 645 F g^{-1} at 1 A g^{-1}.[242] Umair *et al.* synthesized an asymmetric supercapacitor device from PANI@CoNbS composite and PANI@AC composite. The quasi-capacitive performance of the PANI@CoNbS electrode, along with the high specific surface area of the PANI@AC electrode, resulted in an efficient asymmetric device (35 W h kg^{-1}) (Table 3).[243]

4.4. The electrochemical energy-storage performance of MOF/conductive polymers composites and MOF/conductive polymers/TMO or TMS composites

Metal–organic frameworks were prepared from metal ions linked by organic ligands. The connection between metal ions and organic ligands was established through coordination bonds. MOF are porous structures with high specific surface areas, thus providing active sites for electron transport.[278] The redox properties of metals combined with organic ligands offer high potential for energy storage. Two-dimensional metal–organic frameworks provide a shorter path for electron transfer and electrochemical activity. Metal–organic frameworks made of cobalt, zinc, zirconium, and nickel have been reported in supercapacitor studies. Johnson *et al.* synthesized Co-MOF/polyaniline composite by *in situ* oxidative polymerization. The Co-MOF/PANI composite electrode material with a high specific surface area and conductivity recorded 504 F g^{-1} at 1 A g^{-1}.[279] Ebenezer *et al.* investigated the behavior Ni-MOF/polyaniline composite in detail. The electrochemical analyses showed that the specific capacitance of the PANI/Ni-MOF was twice that of polyaniline and Ni-MOF. Despite the faradaic behavior of Ni-MOF and polyaniline, the composite electrode materials had high performance as electroactive materials and retained 99% specific capacitance up to 5000 cycles.[280] Maheshwari *et al.* synthesized copper MOF derived from plastic waste residues. Despite the high specific surface area of the copper metal framework, its conductivity was low. Composites based on

Table 3 The electrochemical data of TMO/CP/C or TMS/CP/C composites

Sample	Stability (cycles)	Specific capacitance (or areal specific capacitance)	Current density (or areal current density)	Reference
Co_3O_4/polyaniline/graphene	94% up to 3000	476 F g^{-1}	2 A g^{-1}	244
MnS/PANI/CNT	85% up to 1000	325 F g^{-1}	1 A g^{-1}	245
$ZnCoO_x$/C–PANI	80% up to 5000	1055 F g^{-1}	1 A g^{-1}	246
PANI–rGO–CoS	90% up to 1000	431 F g^{-1}	0.5 A g^{-1}	247
PANI–rGO–Co_3S_4	81.7% up to 5000	767 F g^{-1}	1 A g^{-1}	248
GO/PANI/$CuCo_2O_4$	84.25% up to 5000	312.72 F g^{-1}	1 A g^{-1}	249
PANI/SnS_2@CNTs	83.6% up to 6000	891 F g^{-1}	20 mV s^{-1}	250
PANI/CNT/e-MoS_2	80% up to 4000	532 F g^{-1}	1 A g^{-1}	251
$NiCo_2S_4$/PANI/CNT	80.13% up to 5000	1290 mF cm^{-1}	2 mA cm^{-1}	252
Cs/CNTs/PANI	87.5% up to 5000	767 F g^{-1}	1 A g^{-1}	253
CS/GM/Fe_3O_4/PANI	99.8% up to 5000	1513.4 F g^{-1}	4 A g^{-1}	254
La_2S_3/PANI/N–rGO	94.87% up to 5000	2311.2 F g^{-1}	5 A g^{-1}	255
$As_3Mo_8V_4$/PANI/rGO	85.7% up to 5000	1295 F g^{-1}	1 A g^{-1}	256
VO_2/CNT@PANI	88.2% up to 5000	354.2 F g^{-1}	0.5 A g^{-1}	257
CuS/C@PANI	89.86% up to 3000	425.53 F g^{-1}	1 A g^{-1}	258
PANI/GO/$CuFe_2O_4$	88% up to 3500	614.76 F g^{-1}	1 A g^{-1}	259
Mn_3O_4/PANI/G	97% up to 3000	1240 F g^{-1}	2 A g^{-1}	260
PANI–GO–Mn_3O_4	89% up to 4000	460 F g^{-1}	1 A g^{-1}	261
MoS_x–PANI@RGO	88% up to 5000	1365 F g^{-1}	1 A g^{-1}	262
CF/Ni_3S_2@PANI	93.4% up to 2500	318 F g^{-1}	1 A g^{-1}	263
$NiSe_2$/rGO/PANI	100% up to 12 000	657.36 C g^{-1}	1 A g^{-1}	264
PANI/nTiO_2/AC	72% up to 10 000	827 F g^{-1}	10 mV s^{-1}	265
NiO/g-C_3N_4/CNTs/TiO_2	—	362.12 F g^{-1}	1 A g^{-1}	266
rGO@Fe_2O_3/CuO/PANI	96% up to 1000	1210 F g^{-1}	1 A g^{-1}	267
α-Fe_2O_3/SnO_2/rGO	98.7% up to 10 000	821 F g^{-1}	1 A g^{-1}	268
CNTs-PANI/$CoNi(PO_4)_2$	100% up to 5000	2136 F g^{-1}	1.5 A g^{-1}	269
PPy/MnO_2/CC	91% up to 5000	324.5 mF cm^{-2}	2.5 mA cm^{-2}	270
CC/MnO_2/PPy	96.46% up to 8000	123.96 F g^{-1}	10 mV s^{-1}	271
g-C_3N_4/V_2O_5/PANI	78% up to 2000	880 F g^{-1}	1 A g^{-1}	272
rGO/PANI/ZnO	97% up to 3000	1546 F g^{-1}	2 mV s^{-1}	273
MoO_3/PPy/rGO	85% up to 6000	412.3 F g^{-1}	0.5 A g^{-1}	274
V_2O_5/PPy/GO	83% up to 3000	750 F g^{-1}	5 A g^{-1}	275
V_2O_5/f-CNT/PPy	83% up to 10 000	1266 mF cm^{-2}	1 mA cm^{-1}	276
MnO_2/PANI–GCN	82% up to 1000	318 F g^{-1}	1 A g^{-1}	277

conductive polymers (polyaniline and polypyrrole) and copper metal–organic framework were designed and synthesized to improve conductivity and increase the electron transfer rate. According to the electrochemical performance results of composites based on conductive polymers and copper metal–organic framework, additional channels for ion transport were created by the addition of conductive polymer.[281] Hybrids of MOF and CP have been synthesized to prevent polymer aggregation and achieve high conductivity and specific surface area. However, the addition of metal oxide increases stability and mechanical strength. Yang *et al.* synthesized a three-component of polyaniline/zinc oxide/cobalt metal organic framework in two steps, as shown in Fig. 11. The high conductivity of conductive polymers, the high specific surface area of the MOF, and the mechanical strength of zinc oxide resulted in efficient hybrid electrode materials with 458.9 F g^{-1} at 1 A g^{-1}.[282]

Boopathiraja *et al.* synthesized a composite of polypyrrole, MOF, and zinc oxide by the hydrothermal method. The supercapacitive behavior was improved by changing the type of conductive polymer (polypyrrole instead of polyaniline), and 1181 F g^{-1} at 1 A g^{-1} was recorded.[283] The g-C_3N_4 is a carbon-based structure where the electron-donating properties of nitrogen accelerate electron transfer. Composites of g-C_3N_4 and CP have been synthesized to prevent the aggregation of two-dimensional g-C_3N_4 structures.[284,285] Fu *et al.* synthesized a quaternary composite of PANI/g-C_3N_4/Ni-MOF/nickel oxide in three steps. First, a composite of PANI and g-C_3N_4 was synthesized through chemical oxidation. Second, it was attached to a nickel MOF, and finally, nickel oxide was injected. The polyaniline in the composite structure prevented the g-C_3N_4 sheets from overlapping, and the metal oxide increased the stability. Therefore, the quaternary composite-based electrode material with high specific surface area, high stability, and multiple active sites showed 2420 F g^{-1} at 5 A g^{-1}.[286] Other carbon materials, including GO, G, and AC, were incorporated as electroactive components in composites of CP, MOF, and CNT. Rani *et al.* synthesized composites based on polyaniline, metal–organic framework, and graphene oxide by the hydrothermal method. The synergistic effect of highly conductive carbon materials, cobalt MOF with multiple active sites, and polyaniline as a plate separator resulted 290 F g^{-1} at 1 A g^{-1}.[287] Some *et al.* first synthesized GO by the Hummers' method to manufacture a metal–organic framework of zinc/rGO, and polypyrrole composite. Then, combined polypyrrole and graphene oxide by a chemical method. Finally, a ternary composite was synthesized by adding imidazole and zinc nitrate to the solution through a hydrothermal method. The ternary composite with multiple sites and high surface area for electron transfer recorded 175 F g^{-1} at 1 A g^{-1}.[288]

4.5. The MXene/CP composites for supercapacitors

MXenes are two-dimensional materials with high surface area. MXenes were synthesized from transition metals, carbides, and nitrides.[289] These materials have advantages, including thermal stability and high mechanical strength, which outperform other 2D materials (graphene). Therefore, MXenes have good performance in sensors, batteries, supercapacitors, and water purification. MXenes have metallic conductivity and hydrophilic properties, which make their performance unique. In other words, MXenes have the properties of being stable like ceramics and conducting like metals. However, MXene sheets tend to aggregate during long cycles. Therefore, MXene-based composites were designed and synthesized. The conductive polymer is placed between the MXene plates in MXene/CP composites to prevent the plates from agglomerating. Jin *et al.* synthesized the MXene/polyaniline composite by

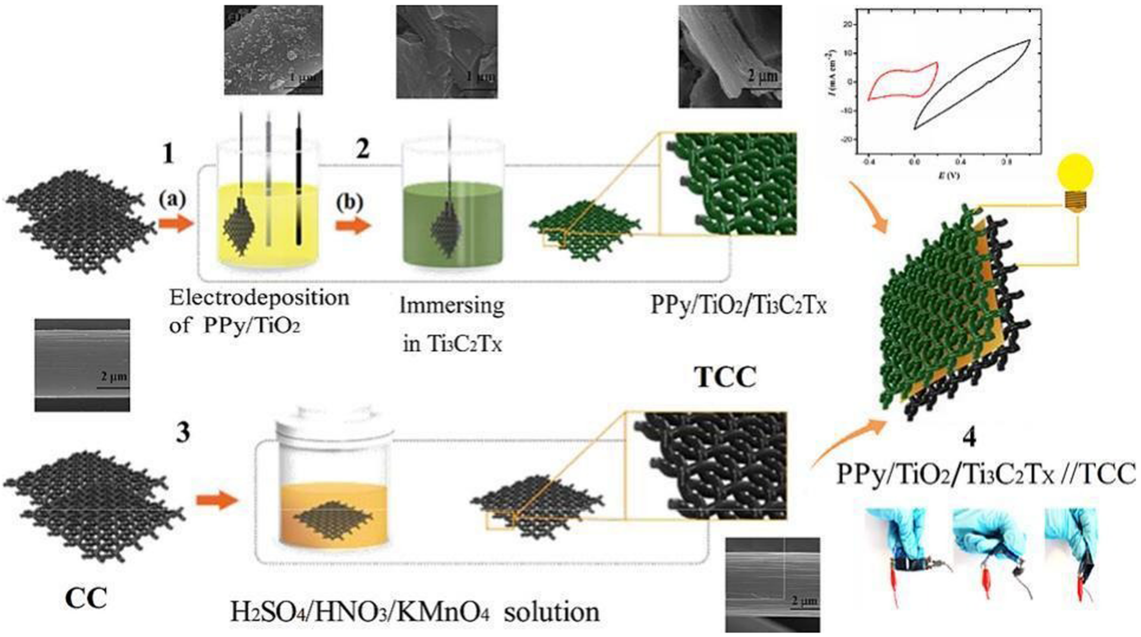

Fig. 11 A general scheme for the preparation of ZnO_2/PANI/Co-MOF composite.

a hydrothermal method. The BET analyses showed that the specific surface area increased with the addition of MXene. Therefore, the ion diffusion was facilitated. Polyaniline acted as a coupling agent between the MXene layers in the composite, thus facilitating charge transfer between the layers. The MXene/PANI showed 563 F g^{-1} at 0.5 A g^{-1}.[290] Singh *et al.* first prepared polyaniline through *in situ* polymerization and $Ti_3C_2T_x$ by the mild-etching method. Then, the composite based on $Ti_3C_2T_x$ and polyaniline was synthesized through the polymerization (Fig. 12). The graphite current collector was used to investigate the electrochemical performance of $Ti_3C_2T_x$/PANI. This study was compared with similar studies conducted with other current collectors (Ni and C cloth). The use of a graphite current collector for $Ti_3C_2T_x$/polyaniline composite resulted in reduced resistance and increased stability. The $Ti_3C_2T_x$/polyaniline composite showed 854 F g^{-1} at 1 A g^{-1}.[291]

Zhang *et al.* synthesized (PANI)/MXene composites by the *in situ* polymerization. This synthesis method, the high surface area of MXene increases the electronegativity, which promotes the polymerization of aniline on the MXene surface. The high surface area of MXene improved the electrochemical activity of the PANI/MXene composite. The asymmetric device of (PANI)/MXene recorded 11.25 W h kg^{-1}.[292] Wang *et al.* synthesized multilayer MXene. Functional of MXene provided conditions for the synthesis of composites with different ratios of MXene and polyaniline. The functional groups of MXene provided active nucleation sites for the growth of polyaniline on MXene. The MXene/PANI electrode material with the optimal ratio showed 222 F g^{-1}.[293] The MXene/polyaniline composite can be grown on carbon fabric, thereby preventing the accumulation of MXene. Yang and co-workers grew MXene and polyaniline-based composites on carbon cloth. The synthesis and design

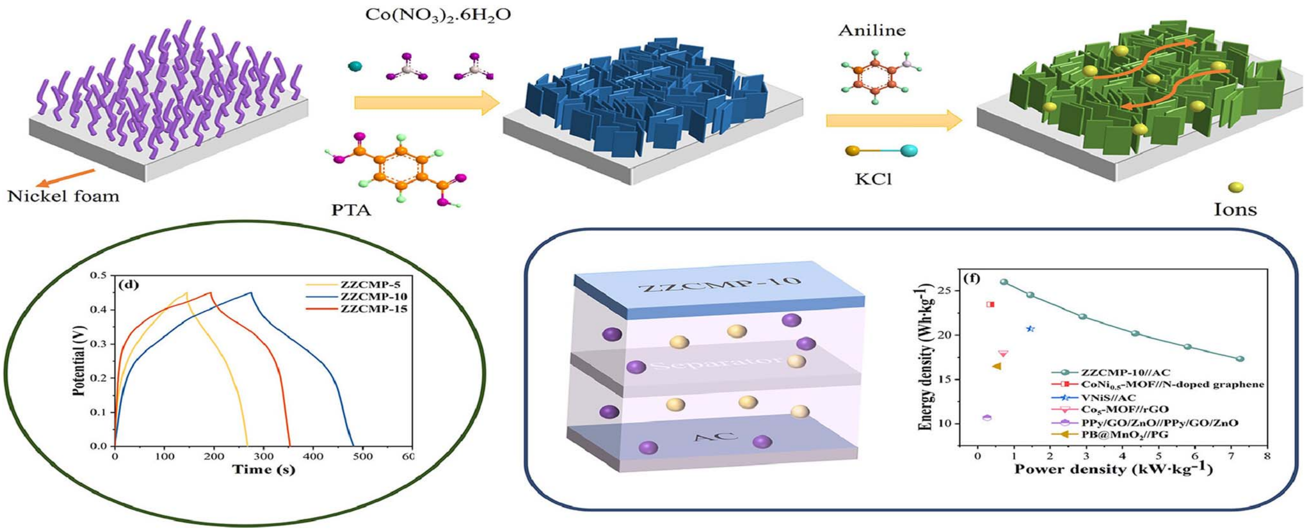

Fig. 12 A general scheme for the preparation of PPy/TiO_2/$Ti_3C_2T_x$ composite.

Table 4 The electrochemical data of MXene/CP composites

Sample	Stability (cycles)	Specific capacitance (or areal specific capacitance)	Current density (or areal current density)	Reference
Ti_2CT_x@polyaniline	97.54% up to 10 000	635 F g^{-1}	1 A g^{-1}	298
MXene–CNT/PANI	93% up to 10 000	429.4 F g^{-1}	1 A g^{-1}	299
MXene/PANI	98% up to 10 000	336 F g^{-1}	1 A g^{-1}	300
MXene/polyaniline	84.6% up to 5000	645.7 F g^{-1}	1 A g^{-1}	301
MXene/PANI	86.5% up to 5000	523.8 F g^{-1}	1 A g^{-1}	302
MXene/PANI	86% up to 5000	190.8 F g^{-1}	1 A g^{-1}	303
Ti_3C_2/PANI-NTs-1	86% up to 4000	596.6 F g^{-1}	1 A g^{-1}	304
MXene/PANI	81.6% up to 10 000	361.9 mF cm^{-3}	6 mA cm^{-3}	305
$Ti_3C_2T_x$/PANI	96.4% up to 10 000	385 F g^{-1}	10 V s^{-1}	306
MXene/PANI	89.4% up to 9000	483.1 F g^{-1}	1 A g^{-1}	307
PANI@MXene–CNTs	92% up to 10 000	463 F g^{-1}	5 mV s^{-1}	308
MXene/PANI	71.6% up to 3000	327 F g^{-1}	1 A g^{-1}	309
$Ti_3C_2T_x$ MXene/polypyrrole	86.8% up to 6000	563.8 F g^{-1}	0.5 A g^{-1}	310
Ti_3C_2–MXene/polypyrrole	73.68% up to 4000	458 F g^{-1}	2 mV s^{-1}	311
PPy@MXHCNF	92.8% up to 10 000	567.5 F g^{-1}	1 A g^{-1}	312
Ti_3C_2 MXenes/polypyrrole	83.33% up to 4000	184.36 F g^{-1}	2 mV s^{-1}	313
PANI/MXene	86% up to 10 000	322 F g^{-1}	0.5 A g^{-1}	314

of a 2D/0D/1D structure improved the electron transfer rate and composite homogeneity. Therefore, the composite grown on carbon cloth showed areal specific capacitance 1347 mF cm^{-2}.[294] Bae *et al.* synthesized ($Ti_3C_2T_x$)/polyaniline composites by Ti_3AlC_2 etching followed *via* polymerization. The electrochemical analysis of the ($Ti_3C_2T_x$)/polyaniline composite showed 458.3 F g^{-1} at 5 mV s^{-1}.[295] Wang *et al.* sulfonated polyaniline to prepare a 3D composite structure based on PANI and MXene. Sulfonation of polyaniline accelerated the redox reaction and also caused the disordered growth of polyaniline on MXene. The irregular growth of polyaniline between the MXene sheets resulted in a three-dimensional structure that facilitates the ions movement. The composite based on MXene and PANI showed 512.45 F g^{-1}.[296] Hou *et al.* synthesized $Ti_3C_2T_x$/polyaniline film by the suction filtration method. The polyaniline increased the spacing of $Ti_3C_2T_x$ sheets as indicated by the chemical analysis. Therefore, the rate of ion transport increased, and the $Ti_3C_2T_x$/polyaniline film as an efficient electroactive material showed 272.5 F g^{-1} at 1 A g^{-1} (Table 4).[297]

5. Conclusion and future prospects

The development of industry and the depletion of fuel resources have been discussed as a global challenge. The supercapacitor has been introduced as a suitable technology to replace fossil fuels. Conductive polymers as electrode materials have metallic conductivity and polymer properties simultaneously. The instability of conductive polymers during long cycles is due to the volume change of polymer chains, thus limiting the performance of CP in supercapacitor systems. High-stability hybrid compounds were achieved by preparing composites based on conductive polymers and other electroactive materials. Composites prepared from conductive polymers with C, TMO, MOF, and TMS were reported as a high-performance hybrid compound in recent studies. Despite the optimal performance of composites based on conductive polymers, conductive polymers have low processability and cannot be used in large quantities in wide areas. Therefore, some important challenges related to conductive polymer-based composites include industrial scalability and standardization of mass production, and the toxic effects of conductive polymers on the environment, which have prevented the widespread adoption of polymer-based composites as electrode materials. In addition, high production cost, material incompatibility, sensitivity to high temperatures, low solubility in solvents, and the inability to process this material directly in the melt state are considered challenges for conductive polymers. Industrial production of conductive polymer-based composites on a scale beyond laboratory environments may result in changes to their electrochemical properties. Therefore, this requires large investments and technological development that may not be economically justified. High production costs may prevent widespread adoption of conductive polymer-based composites in the global market. Researchers' awareness of the advantages and disadvantages of conductive polymer-based composite electrode materials will be effective in the intelligent development of this technology. Much effort and research must be made to achieve high-performance electrode materials of conductive polymer-based composites. Researchers can overcome energy supply constraints in industry by designing and synthesizing conductive polymer-based composites with greater solubility, lower toxicity, and cost-effectiveness.

Conflicts of interest

The authors have no conflict of interest.

Data availability

No primary research results, software or code have been included and no new data were generated or analysed as part of this review.

Acknowledgements

The authors gratefully acknowledge the University of JAIN (Deemed to be University) and University of Nursing for the financial support for this research.

References

1 P. Es' haghi, H. Seddighi, K. Shayesteh and N. Omrani, *Chem. Rev. Lett.*, 2024, **7**, 1042–1052.
2 S. Gautam, S. Rialach, S. Paul and N. Goyal, *RSC Adv.*, 2024, **14**, 14311–14339.
3 O. A. Al-Basri, A. A. Mohammed, A. A. Salman, M. A. Kadhom and E. A. Yousif, *Chem. Res. Technol.*, 2025, **2**, 90–98.
4 N. Norouzi and S. Talebi, *Chem. Rev. Lett.*, 2020, **3**, 38–52.
5 N. Kumar, R. Aepuru, S.-Y. Lee and S.-J. Park, *Mater. Sci. Eng., R*, 2025, **163**, 100932.
6 E. Vessally, R. M. Rzayev, A. A. Niyazova, T. Aggarwal and K. E. Rahimova, *RSC Adv.*, 2024, **14**, 40141–40159.
7 T. Abedin, J. Pasupuleti, J. K. S. Paw, Y. C. Tak, M. Mahmud, M. P. Abdullah and M. Nur-E-Alam, *J. Power Sources*, 2025, **640**, 236769.
8 L. Wenkai, X. Zhiyong and Z. Haodong, *RSC Adv.*, 2024, **14**, 7172–7194.
9 J. Wu, J. Li and X. Yao, *Adv. Funct. Mater.*, 2025, **35**, 2416671.
10 T. H. Karakoc, C. O. Colpan, S. Ekici and O. Yetik, *Journal of Green Energy*, 2025, **22**, 1402.
11 P. Kumar, K. Kumar, N. Adhikary and E. L. Tesfaye, *Sci. Rep.*, 2025, **15**, 13953.
12 M. A. Dar, S. Majid, M. Satgunam, C. Siva, S. Ansari, P. Arularasan and S. R. Ahamed, *Int. J. Hydrogen Energy*, 2024, **70**, 10–28.
13 Y. Wang, T. Xu, K. Liu, M. Zhang, X. M. Cai and C. Si, *Aggregate*, 2024, **5**, e428.
14 P. Gaikwad, N. Tiwari, R. Kamat, S. M. Mane and S. B. Kulkarni, *Mater. Sci. Eng., B*, 2024, **307**, 117544.
15 J. Li, C. Liu, R. Momen, J. Cai, X. Hu, F. Zhu, H. Liu, L. Xu, W. Deng and H. Hou, *Coord. Chem. Rev.*, 2024, **517**, 216018.
16 V. Surendran and V. Thangadurai, *ACS Appl. Energy Mater.*, 2024, **7**, 1873–1881.

17 X. Xu, X. Han, L. Lu, F. Wang, M. Yang, X. Liu, Y. Wu, S. Tang, Y. Hou and J. Hou, *J. Power Sources*, 2024, **603**, 234445.
18 J. Zia and M. Tejaswini, *RSC Adv.*, 2025, **15**, 9055–9080.
19 A. I. Saber, H. K. Dabis, N. M. A. Alsultany, H. M. H. Abdulwahab, A. S. Mansoor, N. S. Abd and F. Alimola, *Chem. Rev. Lett.*, 2025, **8**, 639–658.
20 F. Alimola and N. Arsalani, *J. Alloys Compd.*, 2025, 181190.
21 F. Alimola, N. Arsalani and I. Ahadzadeh, *Mater. Chem. Phys.*, 2024, **319**, 129293.
22 P. Molaiyan, M. Abdollahifar, B. Boz, A. Beutl, M. Krammer, N. Zhang, A. Tron, M. Romio, M. Ricci and R. Adelung, *Adv. Funct. Mater.*, 2024, **34**, 2311301.
23 S. Lan, C. Yu, J. Yu, X. Zhang, Y. Liu, Y. Xie, J. Wang and J. Qiu, *Small*, 2024, 2309286.
24 K. Dissanayake and D. Kularatna-Abeywardana, *J. Energy Storage*, 2024, **96**, 112563.
25 X. Liu, N. Ostrovsky-Snider, M. Lo Presti, T. Kim, G. Guidetti and F. G. Omenetto, *ACS Biomater. Sci. Eng.*, 2024, **10**, 5390–5398.
26 Y. Weng, N. Tan, Z. Cao, B. Huang, B. Lu, H. Liu, X. You, J. Lv, Y. Guo and L. Tang, *J. Energy Storage*, 2025, **118**, 116259.
27 S. Khan, S. Chand and C. Chakraborty, *Chem. Eng. J.*, 2025, 164232.
28 Q. Liu, T. Wang, D. Jia, P. Ren and D. Wu, *Adv. Funct. Mater.*, 2025, 2500016.
29 S. Jha, Y. Qin, Y. Chen, Z. Song, L. Miao, Y. Lv, L. Gan and M. Liu, *J. Mater. Chem. A*, 2025, **13**, 15101–15110.
30 S. B. Aziz, P. O. Hama, D. M. Aziz, N. M. Sadiq, H. J. Woo, M. F. Kadir, R. T. Abdulwahid, B. A. Al-Asbahi, A. A. Ahmed and J. Hassan, *J. Energy Storage*, 2025, **114**, 115841.
31 M. A. Hossain, K. Sheikh, M. S. Islam Sagar, K. R. Hossain, X. Yao, C. Bai and X. Wang, *Chem. Rev. Lett.*, 2023, **6**, 461–478.
32 Z. H. Hussein, F F Karam and N. Rahi Mashkur, *Chem. Rev. Lett.*, 2025, **8**, 128–136.
33 F. Mashkoor, M. Shoeb, S. Zhu, J. Ahmed, S. M. Noh and C. Jeong, *Surf. Interfaces*, 2025, **62**, 106198.
34 S. N. Ndung'u, T. Nyahanga, E. Kinuthia, A. Ndiritu, S. Kirkok and J. Kirimi, *J. Chem. Technol.*, 2025, e229562.
35 G. A. Tafete, N. G. Habtu, M. K. Abera, T. A. Yemata, A. K. Shibeshi and N. W. Kebede, *Sustainable Development Research in Materials and Renewable Energy Engineering: Advancements of Science and Technology*, 2025, pp. 127–157.
36 P. V. Patale, S. R. Mathapati and J. L. Somawanshi, *J. Chem. Lett.*, 2024, **5**, 206–220.
37 J. Khan, A. Ahmed and A. A. Al-Kahtani, *Mater. Adv.*, 2025, **6**, 3344–3354.
38 G. B. Pour and L. F. Aval, *Electrochem. Commun.*, 2025, 107874.
39 M. F. Jimoh, G. S. Carson, M. B. Anderson, M. F. El-Kady and R. B. Kaner, *Adv. Funct. Mater.*, 2025, **35**, 2405569.
40 Z. Zhu, Y. Bu, C. Gu and X. Wang, *J. Eur. Ceram. Soc.*, 2025, 117423.
41 D. Dake, N. Raskar, V. Mane, R. Sonpir, K. Gattu and B. Dole, *Material Science for Future Applications: Emerging Development and Future Perspectives*, 2025.
42 Z. Hou, L. Chang, W. Yang, R. Yang, A. Wei, K. Cai and S. Luo, *J. Energy Storage*, 2024, **100**, 113550.
43 A. Samage, M. Halakarni, H. Yoon and N. S. Kotrappanavar, *Carbon*, 2024, **219**, 118774.
44 M. Goyal, K. Singh and N. Bhatnagar, *Prog. Org. Coat.*, 2024, **187**, 108083.
45 V. Golovakhin, V. I. Litvinova, A. Manakhov, A. R. Latypova, O. N. Novgorodtseva, A. V. Ukhina, A. V. Ishchenko, A. S. Al-Qasim, E. A. Maksimovskiy and A. G. Bannov, *Mater. Today Commun.*, 2024, **39**, 109163.
46 J. E. Ogbu and C. I. Idumah, *Polym.-Plast. Technol. Mater.*, 2024, **63**, 939–974.
47 K. Chattopadhyay, A. Basak, G.-B. Lee, M. Mandal, C. Nah and D. K. Maiti, *ACS Appl. Energy Mater.*, 2024, **7**, 8683–8693.
48 Z. Çıplak, *J. Electron. Mater.*, 2022, **51**, 1077–1088.
49 D. Gui, C. Liu, F. Chen and J. Liu, *Appl. Surf. Sci.*, 2014, **307**, 172–177.
50 A. K. Sharma, Y. Sharma, R. Malhotra and J. Sharma, *Adv. Mater. Lett.*, 2012, **3**, 82–86.
51 N. M. Yousif and M. R. Balboul, *Russ. J. Electrochem.*, 2024, **60**, 1133–1152.
52 D. Geetha, *ECS J. Solid State Sci. Technol.*, 2025, **14**(7), 076002.
53 A. Soleimani, H. G. Taleghani and M. S. Lashkenari, Ternary RGO/PANI/UCNT nanohybrid for high performance electrochemical supercapacitors, *Research Square*, 2024, DOI: 10.21203/rs.3.rs-4589783/v1.
54 K. Batool, M. Rani, S. M. Osman, M. Sillanpää, R. Shafique, S. Khan and M. Akram, *Diamond Relat. Mater.*, 2024, **143**, 110904.
55 B. E. Conway, *Electrochemical Supercapacitors: Scientific Fundamentals and Technological Applications*, Springer Science & Business Media, 2013.
56 Z. S. Iro, C. Subramani and S. Dash, *Int. J. Electrochem. Sci.*, 2016, **11**, 10628–10643.
57 P. Pattathil, N. Sivakumar and T. S. Sonia, Capacitor to Supercapacitor: An Introduction, in *Nanostructured Ceramic Oxides for Supercapacitor Applications*, ed. A. Balakrishnan and K. R. V. Subramanian, CRC Press, Boca Raton, 2014, ch. 1, pp. 1–10.
58 A. González-Banciella, D. Martinez-Diaz, J. Artigas-Arnaudas, M. V. Vázquez, M. Sánchez and A. Ureña, *J. Alloys Compd.*, 2025, 181139.
59 F. Alimola, N. Arsalani and I. Ahadzadeh, *Electrochim. Acta*, 2022, **417**, 140283.
60 S. Sahoo, S. Ratha, C. S. Rout and S. K. Nayak, *J. Mater. Sci.*, 2022, **57**, 4399–4440.
61 V. D. Nithya, *J. Electron. Mater.*, 2025, 1–20.
62 R. Aslani and H. Namazi, *J. Ind. Eng. Chem.*, 2022, **112**, 335–347.
63 R. Aslani and H. Namazi, *React. Funct. Polym.*, 2022, **170**, 105101.

64 U. Okoroanyanwu, A. Bhardwaj and J. J. Watkins, *ACS Appl. Mater. Interfaces*, 2023, **15**, 13495–13507.

65 K. O. Oyedotun and B. B. Mamba, *Inorg. Chem. Commun.*, 2024, 113154.

66 B. Hashemzadeh, L. Edjlali, P. Delir Kheirollahi Nezhad and E. Vessally, *Chem. Rev. Lett.*, 2021, **4**, 232–238.

67 F. Alimola, N. Arsalani and R. Aslani, *J. Organomet. Chem.*, 2025, 123893.

68 R. A. Khellouf, V. Cyriac, C. Bubulinca and V. Sedlarik, *Energy Environ. Mater.*, 2025, e70023.

69 Y. Aishan, Q. Chen, T. Saito and A. Muto, *Mater. Res. Express*, 2025, **12**, 045601.

70 V. Aswathi and P. Sreeja, *J. Colloid Interface Sci.*, 2025, 137637.

71 A. S. Etman, J. Halim and J. Rosen, *J. Energy Storage*, 2022, **52**, 104823.

72 R. Burt, G. Birkett and X. Zhao, *Phys. Chem. Chem. Phys.*, 2014, **16**, 6519–6538.

73 S. B. Aziz, P. O. Hama, R. T. Abdulwahid, D. M. Aziz, P. A. Mohammed, M. H. Hamsan, R. M. Abdullah and M. F. Kadir, *Emergent Mater.*, 2025, 1–26.

74 F. Ran, M. Hu, S. Deng, K. Wang, W. Sun, H. Peng and J. Liu, *RSC Adv.*, 2024, **14**, 11482–11512.

75 A. R. Ferdous, S. S. Shah, A. Hussain, A. A. Mirghni, Y. P. Hardianto and M. A. Aziz, *Sustainable Mater. Technol.*, 2025, e01296.

76 R. Aslani, F. Alimola and N. Arsalani, *J. Alloys Compd.*, 2025, **1033**, 181190.

77 V. Thirumal, B. Babu, J. Kim, K. Yoo and S. H. Lee, *J. Alloys Compd.*, 2025, **1022**, 179956.

78 K. Chinnaiah, K. Kannan, Y.-S. Chen and K. Gurushankar, *J. Phys. Chem. Solids*, 2025, **196**, 112310.

79 F. Ahmad, M. A. Khan, U. Waqas, S. M. Ramay and S. Atiq, *RSC Adv.*, 2023, **13**, 25316–25326.

80 C. I. Awuzie, *Mater. Today: Proc.*, 2017, **4**, 5721–5726.

81 C. Chiang, M. Druy, S. Gau, A. Heeger, E. Louis, A. G. MacDiarmid, Y. Park and H. Shirakawa, *J. Am. Chem. Soc.*, 1978, **100**, 1013–1015.

82 S. C. Rasmussen, *ChemPlusChem*, 2020, **85**, 1412–1429.

83 L. D. Foyle, G. E. Hicks, A. A. Pollit and D. S. Seferos, *J. Phys. Chem. Lett.*, 2021, **12**, 7745–7751.

84 X. Bai, H.-S. Lee, J.-E. Han, H. N. Murthy and S.-Y. Park, *Horticulturae*, 2025, **11**, 612.

85 H. M. Bergman and T. M. Swager, *J. Am. Chem. Soc.*, 2025, **147**, 12392–12396.

86 D. Xiao, B. Sun, Y. Liu, E. Jiao, X. Wang, X. Chen, X. Cheng, K. Guo, K. Yuan and H. Zhang, *Polym. Polym. Compos.*, 2025, **33**, 09673911241304848.

87 M. Hong, P. U. Do, C. H. Lee and Y. D. Park, *Appl. Surf. Sci.*, 2025, **692**, 162679.

88 M. R. Jalali Sarvestani, *Med. Med. Chem.*, 2024, **1**, 84–90.

89 A. M. Soliman, M. Abd El Aleem Ali Ali El-Remaily, M. S. Kamel, A. El-Araby and E. K. Shokr, *Sci. Rep.*, 2025, **15**, 1611.

90 X. Hu, J. A. Lawrence III, J. Mullahoo, Z. C. Smith, D. J. Wilson, C. R. Mace and S. W. Thomas III, *Macromolecules*, 2017, **50**, 7258–7267.

91 L. Ye, H. Ke and Y. Liu, *Trends Chem.*, 2021, **3**, 1074–1087.

92 A. Kausar, *Conducting Polymer Based Nanocomposites*, Elsevier, Cambridge, MA, USA, 2021, pp. 129–156.

93 R. Liu and Z. Liu, *Chin. Sci. Bull.*, 2009, **54**, 2028–2032.

94 S. Yazar, M. B. Arvas and K. Gürkan, *J. Mater. Sci.*, 2024, **59**, 10936–10952.

95 K. Namsheer and C. S. Rout, *RSC Adv.*, 2021, **11**, 5659–5697.

96 Z. Li and L. Gong, *Materials*, 2020, **13**, 548.

97 K. Ajeel and Q. Kareem, *Journal of Basrah Researches (Sciences)*, 2019, **45**, 2.

98 Z. Jabarzadeh, M. R. Jalali Sarvestani, S. Arabi, M. Mahboubi-Rabbani and S. Ahmadi, *Chem. Rev. Lett.*, 2025, **8**, 576–588.

99 S. Khammarnia, J. Saffari and M.-S. Ekrami-Kakhki, *Chem. Rev. Lett.*, 2025, **8**, 741–750.

100 M. J. Vujković, M. Etinski, B. Vasić, B. Kuzmanović, D. Bajuk-Bogdanović, R. Dominko and S. Mentus, *J. Power Sources*, 2021, **482**, 228937.

101 D. Balan, B. Singh, A. Sheokand and D. Mohan, *J. Mater. Sci.: Mater. Electron.*, 2025, **36**, 1–14.

102 A. Hefnawy, J. El Nady, A. Hassan, F. Mahgoub, S. Ebrahim, R. A. Emanfaloty and A. Elshaer, *J. Alloys Compd.*, 2025, **1019**, 179240.

103 E. Avcu Altıparmak, S. Yazar and T. Bal-Demirci, *Small Methods*, 2025, **9**, 2401140.

104 Y. Liu, K. Luo, W. Xing, W. Yin, J. Feng, S. Pi, Z. Kang, J. Liang, L. Tang and W. Tang, *Angew. Chem., Int. Ed.*, 2025, **64**, e202501797.

105 J. Vícha, L. s. Münster, F. Latečka, M. Martínková, Z. Víchová, O. e. Vašíček and P. Humpolíček, *ACS Sustainable Chem. Eng.*, 2025, **13**(22), 8435–8446.

106 K. A. Milakin, O. Taboubi, M. Lhotka, J. Hromádková, J. Hodan, O. Pop-Georgievski and P. Bober, *Emergent Mater.*, 2025, 1–13.

107 A. L. Pang, A. Arsad and M. Ahmadipour, *Polym. Adv. Technol.*, 2021, **32**, 1428–1454.

108 A. Saidfar, M. Alizadeh and S. Pirsa, *J. Chem. Lett.*, 2020, **1**, 39–46.

109 D. Mantione, I. Del Agua, A. Sanchez-Sanchez and D. Mecerreyes, *Polymers*, 2017, **9**, 354.

110 Q. Zeng, X. Liu, L. Wang, S. Li, X. Xie, G. Liu and Z. Liu, *Chem. Phys.*, 2025, **588**, 112488.

111 S. Sindhu, K. N. Rao, S. Ahuja, A. Kumar and E. Gopal, *Mater. Sci. Eng., B*, 2006, **132**, 39–42.

112 L. Zhou, M. Yu, X. Chen, S. Nie, W. Y. Lai, W. Su, Z. Cui and W. Huang, *Adv. Funct. Mater.*, 2018, **28**, 1705955.

113 H. Nam, H. Cho, H. Lee, H. J. Son and C. Yun, *J. Ind. Eng. Chem.*, 2025, **152**, 256–265.

114 A. S. Ghouri, R. Aslam, S. Siddiqui and S. K. Sami, *J. Coat. Technol. Res.*, 2025, 1–19.

115 Y.-H. Kim, S.-H. Lee, J. Noh and S.-H. Han, *Thin Solid Films*, 2006, **510**, 305–310.

116 Y. Jing and H. Okuzaki, *ACS Appl. Polym. Mater.*, 2025, **7**, 4955–4962.

117 J. Carlberg and O. Inganäs, *J. Electrochem. Soc.*, 1997, **144**, L61.

118 J. Chorbacher, J. Klopf, A. Friedrich, M. Fest, J. S. Schneider, B. Engels and H. Helten, *Angew. Chem., Int. Ed.*, 2025, **64**, e202416088.

119 J. Banerjee and K. Dutta, *Chem. Pap.*, 2021, 1–13.

120 C. Li, M. Liu, N. G. Pschirer, M. Baumgarten and K. Mullen, *Chem. Rev.*, 2010, **110**, 6817–6855.

121 Z. a. Tan, R. Tang, E. Zhou, Y. He, C. Yang, F. Xi and Y. Li, *J. Appl. Polym. Sci.*, 2008, **107**, 514–521.

122 S. Perumal, R. Atchudan, K. Krukiewicz, A. Banaś, D. R. Kumar, H. Lee and W. Lee, *J. Taiwan Inst. Chem. Eng.*, 2025, **172**, 106103.

123 A. M. Díez-Pascual and A. L. Díez-Vicente, *ACS Appl. Mater. Interfaces*, 2014, **6**, 10132–10145.

124 Y. Guo, R. Liu, L. Zhou, H. Zhao, F. Lv, L. Liu, Y. Huang, H.-W. Zhang, C. Yu and S. Wang, *Nano Today*, 2020, **35**, 100969.

125 L. Wan, H. Zhou, H. Zhou, J. Gu, C. Wang, Q. Liao, H. Gao, J. Wu and X. Huo, *Polymers*, 2025, **17**, 1237.

126 S.-K. Qian, Y.-M. Shen, J.-Z. Shen and G.-P. Cao, *Mater. Today Commun.*, 2025, 112475.

127 D. G. Ballard, A. Courtis, I. M. Shirley and S. C. Taylor, *J. Chem. Soc. Chem. Commun.*, 1983, 954–955.

128 A. Abdulkarim, K.-P. Strunk, R. Bäuerle, S. Beck, H. Makowska, T. Marszalek, A. Pucci, C. Melzer, D. Jänsch and J. Freudenberg, *Macromolecules*, 2019, **52**, 4458–4463.

129 K.-P. Strunk, A. Abdulkarim, S. Beck, T. Marszalek, J. Bernhardt, S. Koser, W. Pisula, D. Jänsch, J. Freudenberg and A. Pucci, *ACS Appl. Mater. Interfaces*, 2019, **11**, 19481–19488.

130 B. Ikizer, C. W. Lawton and N. Orbey, *Polymer*, 2021, **228**, 123945.

131 S. Cai, D. Yan, X. Chen, H. Yang, C. Chen, X. Li, Y. Yan and H. Ren, *Polym. Compos.*, 2024, **45**, 1391–1404.

132 J. Banerjee, K. Dutta, M. A. Kader and S. K. Nayak, *Polym. Adv. Technol.*, 2019, **30**, 1902–1921.

133 Y. Huang, H. Li, Z. Wang, M. Zhu, Z. Pei, Q. Xue, Y. Huang and C. Zhi, *Nano Energy*, 2016, **22**, 422–438.

134 A. R. Peringath, M. A. Bayan, M. Beg, A. Jain, F. Pierini, N. Gadegaard, R. Hogg and L. Manjakkal, *J. Energy Storage*, 2023, **73**, 108811.

135 W. Luo, Y. Ma, T. Li, H. K. Thabet, C. Hou, M. M. Ibrahim, S. M. El-Bahy, B. B. Xu and Z. Guo, *J. Energy Storage*, 2022, **52**, 105008.

136 C. Zhao, X. Jia, K. Shu, C. Yu, G. G. Wallace and C. Wang, *J. Mater. Chem. A*, 2020, **8**, 4677–4699.

137 M. Vinayagam, R. S. Babu, A. Sivasamy and A. de Barros, *Diamond Relat. Mater.*, 2025, **154**, 112165.

138 F. Li, J. Shi and X. Qin, *Chin. Sci. Bull.*, 2010, **55**, 1100–1106.

139 F. Liu, H. Ge, F. Gao, J. Li, M. Li, Y. Liu, J. Zhang, M. Li, Y. Wang and M. Zhu, *Batteries Supercaps*, 2025, 2500063.

140 T. M. Alharbi, *J. Taibah Univ. Sci.*, 2024, **18**, 2310885.

141 D. K. Patel, S.-Y. Won, T. V. Patil, S. D. Dutta, K.-T. Lim and S. S. Han, *Int. J. Biol. Macromol.*, 2024, **265**, 131025.

142 A. Bozeya, Y. F. Makableh, L. A. Al-Mezead and R. Abu-Zurayk, *Polym. Bull.*, 2024, **81**, 1707–1727.

143 S. Simon and L. V. Theresa, *Mater. Adv.*, 2025, **6**, 2002–2015.

144 S. Huang, D. Bi, Y. Xia and H. Lin, *ACS Appl. Energy Mater.*, 2023, **6**, 856–864.

145 A. K. Tawade, S. N. Tayade, D. P. Dubal, S. S. Mali, C. K. Hong and K. K. K. Sharma, *Chem. Eng. J.*, 2024, **492**, 151843.

146 M. Ates and C. Alperen, *Iran. Polym. J.*, 2023, **32**, 1241–1255.

147 H. Khanari, M. S. Lashkenari and H. Esfandian, *Int. J. Hydrogen Energy*, 2024, **68**, 27–34.

148 A. Umar, F. Ahmed, N. Ullah, S. A. Ansari, S. Hussain, A. A. Ibrahim, H. Qasem, S. A. Kumar, M. A. Alhamami and N. Almehbad, *Electrochim. Acta*, 2024, **479**, 143743.

149 C. Arumugam, S. K. Kandasamy, K. Gunasekaran, K. Somasundaram and K. P. Eswaramoorthi, *AIP Conf. Proc.*, 2021, **2387**, 090003.

150 S. S. Suranshe, A. Patil, T. Deshmukh and J. Chavhan, *Electrochim. Acta*, 2023, **450**, 142277.

151 S. Porgar, *Chem. Res. Technol.*, 2025, **2**, 170–181.

152 R. Aslani and H. Namazi, *Int. J. Pharm.*, 2023, **636**, 122804.

153 X. Liang, L. Zhao, Q. Wang, Y. Ma and D. Zhang, *Nanoscale*, 2018, **10**, 22329–22334.

154 M. Al-Badri and M. Albdiry, *J. Mater. Sci.: Mater. Electron.*, 2022, **33**, 675–682.

155 A. Aphale, K. Maisuria, M. K. Mahapatra, A. Santiago, P. Singh and P. Patra, *Sci. Rep.*, 2015, **5**, 14445.

156 L. Xu, M. Jia, Y. Li, S. Zhang and X. Jin, *RSC Adv.*, 2017, **7**, 31342–31351.

157 M. R. Jalali Sarvestani and P. Gholami Dastnaei, *Med. Med. Chem.*, 2024, **1**, 31–35.

158 A. B. Adam, M. Y. Abubakar and D. Abubakar, *Med. Med. Chem.*, 2024, **1**, 115–128.

159 S. Abrahi Vahed, *Med. Med. Chem.*, 2024, **1**, 14–19.

160 R. A. Omer, A. Sdiq, A. F. Qader, M. Salih, E. Abdulkareem, H. Ismail, R. Rashid and U. Raheja, *Chem. Rev. Lett.*, 2025, **8**, 612–627.

161 S. Sharanappa, S. Vijaykumar, D. Suresh, A. B. Shbil, H. Ganesha, S. Veeresh, Y. Nagaraju and H. Devendrappa, *J. Energy Storage*, 2023, **74**, 109371.

162 C. Zhou, G. Liu, F. Wang, H. Liu, J. Nai, J. Hao, Z. Sui, Z. Yang and W. Xu, *J. Alloys Compd.*, 2024, **992**, 174618.

163 B. Chen, Q. Yang, Y. Yang, J. Chen, B. Yan, Y. Gu, R. Fu and S. Chen, *J. Power Sources*, 2025, **633**, 236407.

164 M. D. Mehare, A. D. Deshmukh and S. Dhoble, *J. Nanosci. Nanotechnol.*, 2020, **20**, 3785–3794.

165 Y. Zou, Y. Bu, X. Zhou, M. Hu and M. Zhang, *Dalton Trans.*, 2025, **54**, 3722–3732.

166 B. Getiren, H. Altınışık, Z. Çıplak, F. Soysal and N. Yıldız, *Synth. Met.*, 2023, **298**, 117451.

167 E. Dhandapani, N. Duraisamy and R. Rajedran, *ACS Appl. Polym. Mater.*, 2023, **5**, 7420–7432.

168 V. Gupta and N. Miura, *J. Power Sources*, 2006, **157**, 616–620.

169 C. Meng, C. Liu and S. Fan, *Electrochem. Commun.*, 2009, **11**, 186–189.

170 X. Wang, Y. Wang, D. Liu, X. Li, H. Xiao, Y. Ma, M. Xu, G. Yuan and G. Chen, *ACS Appl. Mater. Interfaces*, 2021, **13**, 30633–30642.

171 S.-Y. Lee, J.-I. Kim and S.-J. Park, *Energy*, 2014, **78**, 298–303.

172 A. ur Rahman, H. Noreen, Z. Nawaz, J. Iqbal, G. Rahman and M. Yaseen, *New J. Chem.*, 2021, **45**, 16187–16195.

173 A. Shokry, M. Karim, M. Khalil, S. Ebrahim and J. El Nady, *Sci. Rep.*, 2022, **12**, 11278.

174 A. K. Thakur, M. Majumder, R. B. Choudhary and S. N. Pimpalkar, *IOP Conf. Ser.: Mater. Sci. Eng.*, 2016, **149**, 012166.

175 A. Alabadi, S. Razzaque, Z. Dong, W. Wang and B. Tan, *J. Power Sources*, 2016, **306**, 241–247.

176 X. Lu, H. Dou, C. Yuan, S. Yang, L. Hao, F. Zhang, L. Shen, L. Zhang and X. Zhang, *J. Power Sources*, 2012, **197**, 319–324.

177 J. Melo, E. N. Schulz, C. Morales-Verdejo, S. Horswell and M. Camarada, *Int. J. Electrochem. Sci.*, 2017, **12**, 2933–2948.

178 Y. He, X. Ning and L. Wan, *Polym. Bull.*, 2022, **79**, 9075–9091.

179 M. Barakzehi, M. Montazer, F. Sharif, T. Norby and A. Chatzitakis, *Electrochim. Acta*, 2019, **305**, 187–196.

180 Q. Wang, H. Wang, D. Liu, P. Du and P. Liu, *Synth. Met.*, 2017, **231**, 120–126.

181 X. Jian, H.-m. Yang, J.-g. Li, E.-h. Zhang, L.-l. Cao and Z.-h. Liang, *Electrochim. Acta*, 2017, **228**, 483–493.

182 Z. Zhao and Y. Xie, *J. Power Sources*, 2017, **337**, 54–64.

183 F. M. Omotola, O. O. Olutayo and E. A. Stella, *Chem. Res. Technol.*, 2025, **2**, 99–107.

184 M. F. Shehzad, H. M. Abo-Dief, H. A. Elzilal, T. R. Aldhafeeri, S. K. Ali and M. Faizan, *J. Indian Chem. Soc.*, 2025, 101847.

185 V. Shanmugavalli and K. Vishista, *Mater. Res. Express*, 2019, **6**, 045021.

186 Y. Li, Z. Zhang, Y. Chen, H. Chen, Y. Fan, Y. Li, D. Cui and C. Xue, *Appl. Surf. Sci.*, 2020, **506**, 144646.

187 U. Basak, P. Ghosh, D. P. Chatterjee, G. Mahapatra, A. Banerjee and A. K. Nandi, *J. Mater. Chem. A*, 2025, **13**, 7813–7833.

188 B. Senthilkumar, K. V. Sankar, C. Sanjeeviraja and R. K. Selvan, *J. Alloys Compd.*, 2013, **553**, 350–357.

189 S. Panahi and M. Es' haghi, *Can. J. Chem.*, 2018, **96**, 477–483.

190 Z. Li, Y. Sui, J. Qi, F. Wei, Y. He, Q. Meng, Y. Ren, X. Zhang, Z. Zhan and Z. Sun, *Compos. Interfaces*, 2020, **27**, 631–644.

191 P. S. Shukla, A. Agrawal, A. Kumar, A. Gaur and G. D. Varma, *Journal of Energy Storage*, 2025, **105**, 114782.

192 C. Pan, Z. Liu, W. Li, Y. Zhuang, Q. Wang and S. Chen, *J. Phys. Chem. C*, 2019, **123**, 25549–25558.

193 S. Rajkumar, E. Elanthamilan, J. P. Merlin, I. J. D. Priscillal and I. S. Lydia, *Sustainable Energy Fuels*, 2020, **4**, 5313–5326.

194 Z. Zhao, L. Zheng, H. Li, Z. He, D. Han, J. Shi, B. Xu and H. Wang, *Nanotechnology*, 2022, **33**, 155606.

195 X. Chen and J. Cai, *Dalton Trans.*, 2022, **51**, 16587–16595.

196 N. Boutaleb, G. M. Al-Senani, S. D. Al-Qahtani, A. Benyoucef and B. D. Alkoudsi, *Colloids Surf., A*, 2025, **718**, 136867.

197 M. N. ur Rehman, T. Munawar, M. S. Nadeem, F. Mukhtar, A. Maqbool, M. Riaz, S. Manzoor, M. N. Ashiq and F. Iqbal, *Ceram. Int.*, 2021, **47**, 18497–18509.

198 S. Sahoo, G. Dhakal, W. K. Kim, Y. R. Lee and J.-J. Shim, *J. Energy Storage*, 2023, **73**, 109061.

199 T. Yu, S. Li, L. Zhang, F. Li, H. Pan and D. Zhang, *J. Energy Storage*, 2024, **87**, 111427.

200 J. Dai, C. Yang, Y. Xu, X. Wang, S. Yang, D. Li, L. Luo, L. Xia, J. Li and X. Qi, *Adv. Mater.*, 2023, **35**, 2303732.

201 M. Madeshwaran, K. Rajni and M. Ulaganathan, *Mater. Today Chem.*, 2024, **42**, 102390.

202 K. Li, Z. Li, J. Cui, B. Zhou, W. Dong, B. Zhang and C. Yang, *ChemistrySelect*, 2024, **9**, e202304564.

203 Y. Ye, X. Guo, Y. Ma, Q. Zhao, Y. Sui, J. Song, W. Ma, P. Zhang and C. Qin, *J. Electroanal. Chem.*, 2021, **897**, 115588.

204 Q. Wu, Y. Zhang, Y. Lin, W. Wei, G. Liu, X. Cui, M. Su, H. Jiang, T. Wu and X. Li, *ACS Appl. Mater. Interfaces*, 2023, **15**, 46971–46981.

205 X. Li, H. Xie, Y. Feng, Y. Qu, L. Zhai, H. Sun, X. Liu and C. Hou, *J. Appl. Polym. Sci.*, 2023, **140**, e54580.

206 R. Nagaraj, K. Aruchamy, D. Mondal, S. K. Nataraj and D. Ghosh, *J. Electroanal. Chem.*, 2019, **851**, 113482.

207 A. S. Almalki, *J. Mater. Sci.: Mater. Electron.*, 2024, **35**, 581.

208 S. Ramesh, K. Karuppasamy, H. Yadav, Y.-J. Lee, A. Sivasamy, A. Kathalingam, H.-S. Kim, J.-H. Kim and H. S. Kim, *J. Energy Storage*, 2023, **67**, 107518.

209 T. Mehmood, A. B. Ali, A. Kumar, S. Gouadria, J. Makasana, S. Ballal, K. Chennakesavulu, J. Nanda, R. Chaudhary and A. D. Oza, *J. Alloys Compd.*, 2025, 180887.

210 M. B. Gholivand, H. Heydari, A. Abdolmaleki and H. Hosseini, *Mater. Sci. Semicond. Process.*, 2015, **30**, 157–161.

211 Z. Hai, L. Gao, Q. Zhang, H. Xu, D. Cui, Z. Zhang, D. Tsoukalas, J. Tang, S. Yan and C. Xue, *Appl. Surf. Sci.*, 2016, **361**, 57–62.

212 Y. Fan, H. Chen, Y. Li, D. Cui, Z. Fan and C. Xue, *Ceram. Int.*, 2021, **47**, 8433–8440.

213 F. S. Omar, A. Numan, N. Duraisamy, M. M. Ramly, K. Ramesh and S. Ramesh, *Electrochim. Acta*, 2017, **227**, 41–48.

214 X. Ren, H. Fan, J. Ma, C. Wang, M. Zhang and N. Zhao, *Appl. Surf. Sci.*, 2018, **441**, 194–203.

215 S. Rajkumar, E. Elanthamilan, J. P. Merlin and A. Sathiyan, *J. Alloys Compd.*, 2021, **874**, 159876.

216 M. Usman, M. Adnan, M. T. Ahsan, S. Javed, M. S. Butt and M. A. Akram, *ACS Omega*, 2021, **6**, 1190–1196.

217 J. Yesuraj, V. Elumalai, M. Bhagavathiachari, A. S. Samuel, E. Elaiyappillai and P. M. Johnson, *J. Electroanal. Chem.*, 2017, **797**, 78–88.

218 A. N. Naveen and S. Selladurai, *Mater. Sci. Semicond. Process.*, 2015, **40**, 468–478.

219 Y. V. Naik, R. Naik, H. Nagaswarupa, J. H. Kim, J.-H. Jung, N. T. N. Truong and G. Koyyada, *Inorg. Chem. Commun.*, 2025, 114808.

220 H. Y. Kalyon, Y. F. Karasan and M. Gencten, *Nanotechnology*, 2025, **36**, 215402.

221 A. Qamar, A. Kumar, F. Alharbi, J. Makasana, M. Rekha, G. S. Kumar, M. A. Al-Anber, S. N. Das, R. R. Chaudhary and A. D. Oza, *J. Indian Chem. Soc.*, 2025, 101771.

222 K. Kavya, K. Kalawat, P. Kour, S. Kour and A. Sharma, *Mater. Res. Bull.*, 2025, **184**, 113270.

223 E. Bukhsh, A. Kumar, A. Yadav, A. S. Alqarni, R. Sharma, G. C. Sharma, V. K. Pandey, S.-C. Kim and V. Mishra, *J. Alloys Compd.*, 2025, **1022**, 179441.

224 N. Awoke, G. Beyene, F. Tolassa, M. Asfaw, P. M. Ejikeme, A. C. Nwanya and F. I. Ezema, *ChemistrySelect*, 2025, **10**, e01289.

225 S. Abirami, E. Kumar, B. Vigneshwaran and P. Vijayalakshmi, *Electrochim. Acta*, 2025, 146512.

226 L. Li, Z. Wei, J. Liang, J. Ma and S. Huang, *Results Chem.*, 2021, **3**, 100205.

227 A. Gamal, M. Shaban, M. BinSabt, M. Moussa, A. M. Ahmed, M. Rabia and H. Hamdy, *Nanomaterials*, 2022, **12**, 817.

228 Q. Chen, F. Xie, G. Wang, K. Ge, H. Ren, M. Yan, Q. Wang and H. Bi, *Ionics*, 2021, **27**, 4083–4096.

229 H. Heydari, M. Abdouss, S. Mazinani, A. M. Bazargan and F. Fatemi, *J. Energy Storage*, 2021, **40**, 102738.

230 A. Mindil, H. Hassan, M. W. Iqbal, A. M. Afzal, N. Amri and N. Hadia, *Mater. Chem. Phys.*, 2023, **306**, 128077.

231 P. Elumalai, J. Charles and L. J. Kennedy, *Ionics*, 2024, **30**, 7397–7420.

232 A. B. Adam, K. M. Mahmood, M. Y. Abubakar and F. S. Umar, *Chem. Res. Technol.*, 2025, **2**, 27–37.

233 J. Wang, G. Xiao, T. Zhang, S. Hao, Z. Jia and Y. Li, *J. Alloys Compd.*, 2021, **863**, 158071.

234 Y. Guo, J. Chang, L. Hu, Y. Lu, S. Yao, X. Su, X. Zhang, H. Zhang and J. Feng, *ChemSusChem*, 2024, **17**, e202301148.

235 K. Yasoda, S. Kumar, M. Kumar, K. Ghosh and S. Batabyal, *Mater. Today Chem.*, 2021, **19**, 100394.

236 M. Premkumar and S. Vadivel, *J. Energy Storage*, 2023, **69**, 107948.

237 N. Nabeel, A. Jain, K. C. Juglan and S. Naeem, *Trans. Electr. Electron. Mater.*, 2025, 1–16.

238 E. Azizi, J. Arjomandi, H. Shi and M. A. Kiani, *J. Energy Storage*, 2024, **75**, 109665.

239 Y. Fu, Y. Dong, X. Zhang, H. Niu, C. Qin and X. Jiang, *J. Mater. Sci.*, 2025, 1–18.

240 S. Aslam, F. Shaheen, R. Ahmad, S. M. Ali and Q. Huang, *J. Energy Storage*, 2024, **85**, 111065.

241 R. Kalpana and P. Subbramaniyan, *Int. Res. J. Multidiscip. Technovation*, 2024, **6**, 40–50.

242 R. R. Atram, V. M. Bhuse, R. G. Atram, C.-M. Wu, P. Koinkar and S. B. Kondawar, *Mater. Chem. Phys.*, 2021, **262**, 124253.

243 A. M. Afzal, M. W. Iqbal, M. Imran, H. Umair, S. M. Wabaidur, E. A. Al-Ammar, S. Mumtaz and E. H. Choi, *ECS J. Solid State Sci. Technol.*, 2023, **12**, 051003.

244 P. Haldar, *J. Mater. Sci.: Mater. Electron.*, 2020, **31**, 7905–7915.

245 S. Hema and D. Geetha, *ECS J. Solid State Sci. Technol.*, 2025, **14**, 051006.

246 B. Zhou, Z. Li, D. Qin, Q. Zhang, M. Yu and C. Yang, *J. Alloys Compd.*, 2023, **956**, 170327.

247 H. Heydari and M. B. Gholivand, *J. Mater. Sci.: Mater. Electron.*, 2017, **28**, 3607–3615.

248 A. G. Tabrizi, N. Arsalani, Z. Naghshbandi, L. S. Ghadimi and A. Mohammadi, *Int. J. Hydrogen Energy*, 2018, **43**, 12200–12210.

249 S. Verma, V. K. Pandey and B. Verma, *Synth. Met.*, 2022, **286**, 117036.

250 Z. Zhang, L. Feng, P. Jing, X. Hou, G. Suo, X. Ye, L. Zhang, Y. Yang and C. Zhai, *J. Colloid Interface Sci.*, 2021, **588**, 84–93.

251 M. Jasna, M. M. Pillai, A. Abhilash, P. Midhun, S. Jayalekshmi and M. Jayaraj, *Carbon Trends*, 2022, **7**, 100154.

252 X. Cheng, D. Wang, H. Ke, Y. Li, Y. Cai and Q. Wei, *Compos. Commun.*, 2022, **30**, 101073.

253 X. Hong, X. Wang, Y. Li, C. Deng and B. Liang, *Electrochim. Acta*, 2022, **403**, 139571.

254 M. G. Hosseini, E. Shahryari and P. Yardani Sefidi, *J. Appl. Polym. Sci.*, 2021, **138**, 50976.

255 M. Sadiq, M. Islam, M. Moharam, E. A. M. Saleh and S. U. Asif, *J. Mater. Sci.: Mater. Electron.*, 2024, **35**, 1011.

256 Y. Song, Z. Su, Z. Zhao, S. Lin and D. Wang, *Ceram. Int.*, 2021, **47**, 21367–21372.

257 C. Chen, S. Wei, Q. Zhang, H. Yang, J. Xu, L. Chen and X. Liu, *J. Colloid Interface Sci.*, 2024, **664**, 53–62.

258 Q. Liu, S. Zhang and Y. Xu, *Nanomaterials*, 2020, **10**, 1034.

259 A. K. Ghasemi, M. Ghorbani, M. S. Lashkenari and N. Nasiri, *Electrochim. Acta*, 2023, **439**, 141685.

260 P. Haldar, S. Biswas, V. Sharma, A. Chowdhury and A. Chandra, *Appl. Surf. Sci.*, 2019, **491**, 171–179.

261 R. Boddula, R. Bolagam and P. Srinivasan, *Ionics*, 2018, **24**, 1467–1474.

262 S. P. Lonkar, V. Gupta, S. M. Alhassan and A. Schiffer, *Energy Storage*, 2023, **5**, e416.

263 L. Wang, M. Bo, Z. Guo, H. Li, Z. Huang, H. Che, Z. Feng, Y. Wang and J. Mu, *J. Colloid Interface Sci.*, 2020, **577**, 29–37.

264 E. Harini, D. Rani, M. Afshan, M. Pahuja, N. Chaudhary, S. Rani, S. A. Siddiqui, S. Das, S. Sharangi and R. Ghosh, *Chem. Eng. J.*, 2024, **498**, 155112.

265 G. Singh, Y. Kumar and S. Husain, *Energy Technol.*, 2023, **11**, 2200931.

266 N. Farooq, P. Kallem, M. I. Khan, A. M. Qureshi, A. Shanableh and A. U. Rehman, *J. Mater. Res. Technol.*, 2023, **26**, 7127–7136.

267 T. Abdullah, S. I. Shamsah, I. A. Shaaban, M. Akhtar and S. Yousaf, *Synth. Met.*, 2023, **299**, 117472.

268 M. Geerthana, S. Prabhu, S. Harish, M. Navaneethan, R. Ramesh and M. Selvaraj, *J. Mater. Sci.: Mater. Electron.*, 2022, **33**, 8327–8343.

269 M. R. Abdul Karim, W. Shehzad, M. Atif, E. u. Haq and Z. Abbas, *Energy Environ.*, 2024, 0958305X231221260.

270 Y. Chen, H. He, M. Liu, H. Xu, H. Zhang, X. Zhu and D. Yang, *Nanomaterials*, 2025, **15**, 641.

271 S. Ma, W. Wang, R. Huang, J. Hou, X. Wang, X. Che, Q. Ren, Y. Li and C. Hou, *Appl. Organomet. Chem.*, 2024, **38**, e7497.

272 V. Aswathi and P. Sreeja, *J. Energy Storage*, 2025, **107**, 114993.

273 S. Abbas, Z. M. Elqahtani, G. Yasmeen, S. Manzoor, S. Manzoor, M. Al-Buriahi, Z. Alrowaili and M. N. Ashiq, *J. Korean Ceram. Soc.*, 2023, **60**, 127–140.

274 H. Deng, J. Huang, Z. Hu, X. Chen, D. Huang and T. Jin, *ACS Omega*, 2021, **6**, 9426–9432.

275 P. Asen and S. Shahrokhian, *Int. J. Hydrogen Energy*, 2017, **42**, 21073–21085.

276 J. P. Jyothibasu, M.-Z. Chen, Y.-C. Tien, C.-C. Kuo, E.-C. Chen, Y.-C. Lin, T.-C. Chiang and R.-H. Lee, *Catalysts*, 2021, **11**, 980.

277 P. Chahal, S. L. Madaswamy, S. C. Lee, S. M. Wabaidur, V. Dhayalan, V. K. Ponnusamy and R. Dhanusuraman, *Fuel*, 2022, **330**, 125531.

278 Z. Qin, Y. Xu, L. Liu, M. Liu, H. Zhou, L. Xiao, Y. Cao and C. Chen, *RSC Adv.*, 2022, **12**, 29177–29186.

279 R. Srinivasan, E. Elaiyappillai, E. J. Nixon, I. S. Lydia and P. M. Johnson, *Inorg. Chim. Acta*, 2020, **502**, 119393.

280 T. Ebenezer, I. Johnson, W. Galeb and J. S. K. Arockiasamy, *Electrochim. Acta*, 2024, **507**, 145130.

281 P. Dubey, V. Shrivastav, S. Sundriyal and P. H. Maheshwari, *ACS Appl. Nano Mater.*, 2024, **7**, 18554–18565.

282 D. Qin, B. Zhou, Z. Li and C. Yang, *J. Mol. Struct.*, 2024, **1309**, 138140.

283 A. Revathi, D. J. Williams, D. Sudha and R. Boopathiraja, *J. Mater. Sci.: Mater. Electron.*, 2023, **34**, 1175.

284 S.-X. Zhou, X.-Y. Tao, J. Ma, L.-T. Guo, Y.-B. Zhu, H.-L. Fan, Z.-S. Liu and X.-Y. Wei, *Vacuum*, 2018, **149**, 175–179.

285 A. Atta, R. Altuijri, N. Al-Harbi and M. Abdelhamied, *ECS J. Solid State Sci. Technol.*, 2025, **14**, 043015.

286 S. Kumar, P.-H. Weng and Y.-P. Fu, *Mater. Today Chem.*, 2023, **28**, 101385.

287 M. Rani, B. Zaheer, F. Sajid, A. Ibrahim, A. A. Shah and A. D. Chandio, *J. Inorg. Organomet. Polym. Mater.*, 2025, 1–15.

288 N. Saxena, M. P. Bondarde, K. D. Lokhande, M. A. Bhakare, P. S. Dhumal and S. Some, *Chem. Phys. Lett.*, 2024, **856**, 141605.

289 O. Salim, K. Mahmoud, K. Pant and R. Joshi, *Mater. Today Chem.*, 2019, **14**, 100191.

290 Y. Li, P. Kamdem and X.-J. Jin, *J. Alloys Compd.*, 2021, **850**, 156608.

291 N. Tyagi, G. Sharma and M. K. Singh, *Polymer*, 2025, **326**, 128328.

292 X. Wang, D. Zhang, H. Zhang, L. Gong, Y. Yang, W. Zhao, S. Yu, Y. Yin and D. Sun, *Nano Energy*, 2021, **88**, 106242.

293 W. Bai, Z. Yong, S. Wang, X. Wang, C. Li, F. Pan, D. Liang, Y. Cui and Z. Wang, *J. Energy Storage*, 2023, **71**, 108053.

294 W. L. Liu, Y. Q. Guo, T. Lin, H. C. Peng, Y. P. Yu, F. Yang and S. Chen, *J. Alloys Compd.*, 2022, **926**, 166855.

295 T. Chen, M. Li, Y. Li, S. Song, J. Kim and J. Bae, *Mater. Sci. Eng., B*, 2023, **290**, 116354.

296 G. Ma, W. Bai, X. Zhou, X. Guan, S. Zhang, W. Wu, C. Li and S. Wang, *Chem. Eng. J.*, 2024, **496**, 153730.

297 W. Luo, Y. Wei, Z. Zhuang, Z. Lin, X. Li, C. Hou, T. Li and Y. Ma, *Electrochim. Acta*, 2022, **406**, 139871.

298 J. Fu, J. Yun, S. Wu, L. Li, L. Yu and K. H. Kim, *ACS Appl. Mater. Interfaces*, 2018, **10**, 34212–34221.

299 Y.-Z. Cai, Y.-S. Fang, W.-Q. Cao, P. He and M.-S. Cao, *J. Alloys Compd.*, 2021, **868**, 159159.

300 A. VahidMohammadi, J. Moncada, H. Chen, E. Kayali, J. Orangi, C. A. Carrero and M. Beidaghi, *J. Mater. Chem. A*, 2018, **6**, 22123–22133.

301 B. Chen, Q. Song, Z. Zhou and C. Lu, *Adv. Mater. Interfaces*, 2021, **8**, 2002168.

302 T. He, X. Li, B. Sun, L. Lin, F. Guo, G. Diao, Y. Piao and W. Zhang, *RSC Adv.*, 2024, **14**, 13685–13693.

303 Z. Li, J. Li, B. Wu, H. Wei, H. Guo, Z. M. El-Bahy, B. Liu, M. He, S. Melhi and X. Shi, *J. Mater. Sci. Technol.*, 2024, **203**, 201–210.

304 W. Wu, C. Wang, C. Zhao, D. Wei, J. Zhu and Y. Xu, *J. Colloid Interface Sci.*, 2020, **580**, 601–613.

305 A. Zhang, Y. Wang, H. Yu and Y. Zhang, *Materials*, 2025, **18**, 2277.

306 J. Wang, D. Jiang, M. Zhang, Y. Sun, M. Jiang, Y. Du and J. Liu, *J. Mater. Chem. A*, 2023, **11**, 1419–1429.

307 Y. Zou, H. Liu, G. Liu, B. Yang, J. Li, S. Wang, K. Xie, C. Wang and S. Iqbal, *J. Energy Storage*, 2025, **120**, 116373.

308 X. Wu, W. Hu, J. Qiu, B. Geng, M. Du and Q. Zheng, *J. Alloys Compd.*, 2022, **921**, 166062.

309 L. Xu, W. Wang, Y. Liu and D. Liang, *Gels*, 2022, **8**, 798.

310 W. Luo, Y. Sun, Y. Han, J. Ding, T. Li, C. Hou and Y. Ma, *Electrochim. Acta*, 2023, **441**, 141818.

311 D. Wei, W. Wu, J. Zhu, C. Wang, C. Zhao and L. Wang, *J. Electroanal. Chem.*, 2020, **877**, 114538.

312 I. Pathak, D. Acharya, K. Chhetri, P. C. Lohani, T. H. Ko, A. Muthurasu, S. Subedi, T. Kim, S. Saidin and B. Dahal, *Chem. Eng. J.*, 2023, **469**, 143388.

313 W. Wu, D. Wei, J. Zhu, D. Niu, F. Wang, L. Wang, L. Yang, P. Yang and C. Wang, *Ceram. Int.*, 2019, **45**, 7328–7337.

314 S. Maity, S. Bera, A. Kapuria, A. Debnath, S. Das and S. K. Saha, *Mater. Today Chem.*, 2025, **45**, 102690.